

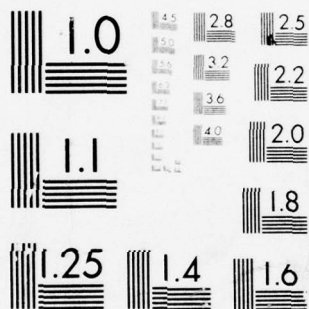
AD-A043 947

DYNAMICS RESEARCH CORP WILMINGTON MASS SYSTEMS DIV F/G 17/9
OPTIMAL SPLINE METHOD WITH APPLICATIONS TO SHIP CLASSIFICATION --ETC(U)
MAR 77 H L STALFORD, C PARK N00014-76-C-1022
R-227U NL

UNCLASSIFIED

1 OF 1
AD
A043947

END
DATE
FILMED
10-77
DDC



MICROCOPY RESOLUTION TEST CHART
NATIONAL BUREAU OF STANDARDS-1963-A

AD A043947

12

AD NO. _____

DDC FILE COPY

DISTRIBUTION STATEMENT A
Approved for public release,
Distribution Unlimited

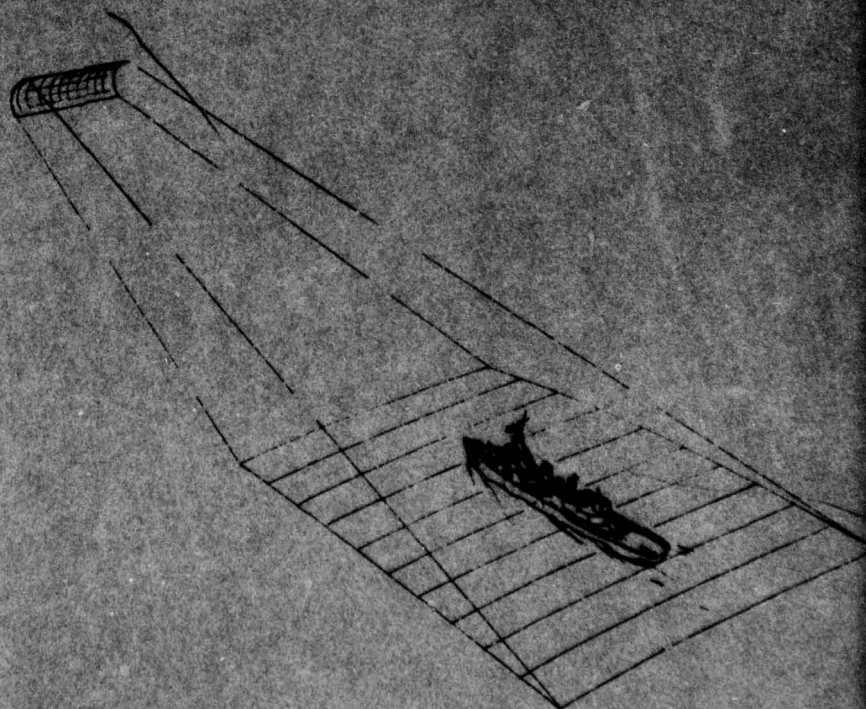
**DYNAMICS
RESEARCH
CORPORATION**



R-227U

**OPTIMAL SPLINE METHOD WITH
APPLICATION TO SHIP CLASSIFICATION
AND TO AIRCRAFT SYSTEM IDENTIFICATION**

MARCH 1977



UNCLASSIFIED

SECURITY CLASSIFICATION OF THIS PAGE (When Data Entered)

REPORT DOCUMENTATION PAGE		READ INSTRUCTIONS BEFORE COMPLETING FORM
1. REPORT NUMBER	2. GOVT ACCESSION NO.	3. RECIPIENT'S CATALOG NUMBER
4. TITLE (and Subtitle) Optimal Spline Method with Applications to Ship Classification and to Aircraft System Identification		5. TYPE OF REPORT & PERIOD COVERED Final Engineering Technical Rept. 23 July 76 - 31 Jan 77
6. AUTHOR(s) Harold L. Stalford and Chan/Park		7. PERFORMING ORG. REPORT NUMBER R-227U
8. PERFORMING ORGANIZATION NAME AND ADDRESS Dynamics Research Corporation 60 Concord Street Wilmington, Mass. 01887		9. CONTRACT OR GRANT NUMBER(s) N00014-76-C-1022
10. CONTROLLING OFFICE NAME AND ADDRESS Office of Naval Research 800 North Quincy Road Arlington, VA 22217		11. PROGRAM ELEMENT, PROJECT, TASK AREA & WORK UNIT NUMBERS 1279
12. MONITORING AGENCY NAME & ADDRESS (if different from Controlling Office) Same		13. REPORT DATE March 1977
		14. NUMBER OF PAGES 75
		15. SECURITY CLASS. (of this report) Unclassified
		16. DECLASSIFICATION/DOWNGRADING SCHEDULE
17. DISTRIBUTION STATEMENT (of this Report) Distribution of this document is unlimited		
18. DISTRIBUTION STATEMENT (of the abstract entered in Block 20, if different from Report)		
19. SUPPLEMENTARY NOTES		
20. KEY WORDS (Continue on reverse side if necessary and identify by block number) Optimal Spline Method Knot and Parameter Optimization Applicability to Ship Classification Applicability to Aircraft System Identification Newton's Gradient Method Quadratic Convergence		
21. ABSTRACT (Continue on reverse side if necessary and identify by block number) This report describes a method for optimal placement of knots in a quadratic spline representation of nonlinear functions. Newton's gradient method is utilized to obtain quadratic convergence of knot locations. Applications to ship classification and to aircraft system identification are presented.		

DD FORM 1 JAN 73 1473

EDITION OF 1 NOV 65 IS OBSOLETE

SECURITY CLASSIFICATION OF THIS PAGE (When Data Entered)

R-227U

OPTIMAL SPLINE METHOD WITH
APPLICATION TO SHIP CLASSIFICATION
AND TO AIRCRAFT SYSTEM IDENTIFICATION

March 1977

Prepared for:
Office of Naval Research
800 North Quincy Road
Arlington, Virginia 22217

Contract No.
N00014-76-C-1022

ACCESSION for	
NTIS	White Section <input checked="" type="checkbox"/>
DDC	Buff Section <input type="checkbox"/>
UNANNOUNCED	
JUSTIFICATION	
BY	
DISTRIBUTION/AVAILABILITY CODES	
SPECIAL	

A

Prepared by:
Harold L. Stalford
Project Engineer

Chan Park
Systems Analyst

Approved by:
Allan Dushman, Manager
Systems Analysis and
Design Department

DYNAMICS RESEARCH CORPORATION
Systems Division
60 Concord Street
Wilmington, Massachusetts 01887

ACKNOWLEDGMENT

This final report is prepared for the Office of Naval Research, Arlington, Virginia under Contract N00014-76-C-1022. This work was performed between July 23, 1976 and January 31, 1977. The technical monitor at ONR is Dr. Stuart Brodsky. Dr. H. L. Stalford, who managed the project, and Dr. Chan Park are the project engineers.

The authors wish to thank their colleague Dr. Harold Schneider for stimulating discussions on aspects of quadratic spline functions.

TABLE OF CONTENTS

	<u>Page</u>
I. INTRODUCTION	1
1.1 Contents and Organization of Report	1
1.2 Study Objectives	2
1.3 Applicability of the Optimal Spline Method to Ship Classification	2
1.4 Applicability of the Optimal Spline Method to Aircraft System Identification	4
II. RESULTS OF AN APPLICATION OF THE OPTIMAL SPLINE METHOD TO SHIP CLASSIFICATION	6
III. RESULTS OF AN APPLICATION OF THE OPTIMAL SPLINE METHOD TO AIRCRAFT SYSTEM IDENTIFICATION	24
IV. MATHEMATICAL DESCRIPTION OF PROBLEM	30
4.1 Time Function Representations	30
4.2 Quadratic Spline Functions	32
4.3 A General Time Function Optimization Problem	35
4.4 Various Cases of the Quadratic Spline Optimization Problem	38
V. SOLUTION TO POSED PROBLEM - AN OPTIMAL SPLINE METHOD	42

Table of Contents (Cont'd)

	<u>Page</u>
VI. ANALYTICAL EXPRESSIONS FOR THE QUANTITIES OF CASE 1	46
6.1 The B Matrix	46
6.2 The $\frac{\partial B}{\partial T_k}$ Matrix	48
6.3 The $\frac{\partial^2 B}{\partial T_k \partial T_n}$ Matrix for $k=n$; $n=1, 2, \dots, m$	49
6.4 The $\frac{\partial^2 B}{\partial T_k \partial T_n}$ Matrix for $k=n+1$, $n=1, 2, \dots, m-1$	51
6.5 The $\frac{\partial^2 B}{\partial T_k \partial T_n}$ Matrix for $k=n+2, \dots, m$; $n=1, 2, \dots, m-2$	52
6.6 The $\underline{\gamma}$ Vector	52
6.7 The $\frac{\partial \underline{\gamma}}{\partial T_k}$ Vector for $k=1, 2, \dots, m$	54
6.8 The $\frac{\partial^2 \underline{\gamma}}{\partial T_k \partial T_n}$ Vector for $n=1, 2, \dots, m$; $k=n, n+1, \dots, m$	55
VII. ANALYTICAL EXPRESSIONS FOR $\frac{\partial E}{\partial T_k}$ and $\frac{\partial^2 E}{\partial T_k \partial T_n}$	56

Table of Contents (Cont'd)

	<u>Page</u>
VIII. ANALYTICAL EXPRESSIONS FOR THE QUANTITIES OF THE SHIP CLASSIFICATION CASE - CASE 2	60
8.1 The B Matrix	60
8.2 The $\frac{\partial B}{\partial T_k}$ Matrix	60
8.3 The $\frac{\partial^2 B}{\partial T_k \partial T_n}$ Matrix for $k=n; n=1, 2, \dots, m$	62
8.4 The $\frac{\partial^2 B}{\partial T_k \partial T_n}$ Matrix for $k=n+1; n=1, 2, \dots, m-1$	63
8.5 The $\frac{\partial^2 B}{\partial T_k \partial T_n}$ Matrix for $k=n+2, \dots, m; n=1, 2, \dots, m-2$	64
8.6 The $\underline{\delta}$ Vector	65
8.7 The $\frac{\partial \underline{\delta}}{\partial T_k}$ Vector for $k=1, 2, \dots, m$	65
8.8 The $\frac{\partial^2 \underline{\delta}}{\partial T_k \partial T_n}$ Vector for $n=1, 2, \dots, m; k=n, n+1, \dots, m$	66
IX. ANALYTICAL EXPRESSIONS FOR THE QUANTITIES OF CASES 3-6	68
9.1 The B Matrix for Case 5	68
9.2 The $\underline{\delta}$ Vector for Case 5	68

Table of Contents (Cont'd)

	<u>Page</u>
X. PROCEDURE FOR STARTING ESTIMATES OF KNOTS	70
10.1 A Procedure for Estimating the Minimum Number of Knots	70
10.2 A Starting Estimates Procedure for the Knot Locations	70
XI. CONCLUSIONS	72
REFERENCES	74

LIST OF FIGURES

<u>Figure</u>		<u>Page</u>
2-1	Block Diagram of DRC's Ship Classification Approach	7
2-2	IRFP Results of Run No. 38/Pass No. 8 on the U.S.S. BARNEY	8
2-3	IRFP Results of Run No. 40/Pass No. 6 on the U.S.S. BARNEY	9
2-4	IRFP Results of Run No. 32/Pass No. 1 on the U.S.S. DAHLGREN	10
2-5	IRFP Results of Run No. 44/Pass No. 1 on the ESSO DENMARK Tanker	11
2-6	Broadside Drawing of the U.S.S. BARNEY (DDG-6)	13
2-7	Broadside Drawing of the U.S.S. DAHLGREN (DLG-12)	13
2-8	ESSO DENMARK Tanker, Length = 677 feet, 49.2 ft. Divisions	14
2-9	Optimal Spline Method Results of Run No. 38/Pass No. 8	15
2-10	Optimal Spline Method Results of Run No. 40/Pass No. 6	16
2-11	Optimal Spline Method Results of Run No. 32/Pass No. 1	17
2-12	Optimal Spline Method Results of Run No. 44/Pass No. 1	18
3-1	Optimal Spline Method Application to Angle of Attack Data	25
3-2	Optimal Spline Method Application to Sideslip Angle Data	26
3-3	Equally Spaced Knots Results of Angle of Attack Data	27
3-4	Equally Spaced Knots Results of Sideslip Angle Data	28

LIST OF TABLES

<u>Table</u>		<u>Page</u>
2-1	Comparison of Optimal Spline Knot Locations	20
2-2	Comparison of Optimal Spline Coefficient Values	21
2-3	Comparison of Least-Squares Error Between Optimally Located Knots and Equally Spaced Knots	22

CHAPTER I

INTRODUCTION

1.1 Contents and Organization of Report

Chapter I contains the study objectives and a discussion of the applicability of the newly developed Optimal Spline Method to ship classification and to the system identification of aircraft nonlinear aerodynamic flight regimes. Summarized in Chapters II and III are its successful application to ship classification work and to an on going aircraft identification study[†]. A detailed mathematical development of the Optimal Spline Method is derived in Chapters IV-X. Chapter IV contains a mathematical description of the problem investigated in the study. Six different cases of the problem are discussed in Section 4.4. The Optimal Spline Method is derived in Chapter V as a solution to the posed problem of Chapter IV. The analytical expressions for the quantities of Case 1 (i.e. the case applicable to aircraft system identification) are derived in Chapters VI and VII. The analytical expressions for the ship classification case (i.e. Case 2) are derived in Chapter VIII. Cases 3-6 are treated in Chapter IX. The procedure that determines the starting estimates of the knots and their locations is described in Chapter X. Chapter XI gives the conclusions.

[†]Study to Develop and Apply Nonlinear State Estimation and Parameter Identification Techniques to the High Angle of Attack/Sideslip Flight Regime of Conventional Aircraft and to the Hover and Low-Speed Flight Regimes of V/STOL Aircraft. Contract No. N62269-76-C-0342, Naval Air Development Center, Warminster, Pennsylvania 18974.

1.2 Study Objectives

A nonlinear function can be chopped into subarcs having small nonlinearities which can be adequately represented by simple spline functions. The domain of a subarc is called a spline region and a point joining one spline region with an adjacent one is called a knot. The piecewise combination of the simple spline functions that fit the subarcs is a spline representation of the nonlinear function. Spline representations can closely approximate the nonlinearities of any function. The goodness of fit depends on the number of spline regions and on the location of the knots. The first objective of this study is to derive an automated method that minimizes the number of spline regions and optimizes the locations of the knots to provide an adequate fit of a given nonlinear function. This has been accomplished by the development of the Optimal Spline Method discussed herein. The second objective is to apply the derived automated method to two important applications. This objective has been accomplished by the successful application of the Optimal Spline Method to ship classification and to system identification of aircraft nonlinear aerodynamic flight regimes.

1.3 Applicability of the Optimal Spline Method to Ship Classification

A major technological area challenging our U.S. Fleet is the over-the-horizon detection, classification and targeting of surface ships. The introduction of weapons like the HARPOON, the TOMAHAWK, and the ALCM have brought about new requirements in ocean surveillance. Active and passive sensors are required to provide beyond the horizon knowledge of all vessels under all weather and communication conditions.

A large gap in surveillance capability currently exists in bad weather for non-communicating targets. The high range resolution radar system is a candidate having great potential to fill this gap. Current technology allows the existence of radar systems capable of obtaining surface ship signatures (stern-bow profiles) having classification potential^[1]. Accordingly, identifying a ship signature is largely a software problem. This report provides a very important contribution to this area by presenting a new technique - an Optimal Spline Method - which generates the independent features of a ship signature for classification purposes.

The integrated signal returns of a high range resolution radar system provide data from which the radar cross-section per range cell of a ship can be estimated. Radar cross-section is a measure of the amount of a ship's superstructure contained in a range cell. Consequently, a graph of the radar cross-sections per range cell drawn over a ship's length (i.e., a stern-bow profile) provides a means for classifying ships. The stern-bow profiles are the signatures for ship classification. The separate superstructure masses provide peaks in the profile while the absence of superstructure appears as valleys. An automated technique is needed for determining the number of separate superstructure masses, their separation from each other, their locations and their extended widths. These are the independent features of a ship's stern-bow radar cross-section profile. The Optimal Spline Method is an automated technique that fulfills this need.

Stern-bow profiles of ships lend themselves well to quadratic spline representations. Quadratic spline functions have the flexibility to fit any ship's stern-bow profile and, most importantly, they have coefficients that represent the independent features. These functions are mathematically described in Section 4.2. The spline coefficients provide the features for pattern recognition, and they are equal to the number of spline regions.

The problem of identifying a pattern increases exponentially with the number of features. Each set of data contains a fixed number of independent features. If too many spline regions are used the independent features are distributed into a higher number of spline coefficients. In this case the set of spline coefficients form a dependent set of features, making the classification problem unnecessarily complex. An independent set of features can be determined by minimizing the number of spline regions. This can be accomplished by optimizing on the locations of the spline regions for each fixed number of knots and by minimizing the number of knots. This is precisely what the Optimal Spline Method accomplishes.

1.4 Applicability of the Optimal Spline Method to Aircraft System Identification

The inability of empirical and theoretical techniques to accurately predict the nonlinear aerodynamics of the high angle of attack/sideslip domain for conventional aircraft and the propulsion induced aerodynamics on V/STOL aircraft has spurred interest in extracting these effects from actual flight data. Efforts to develop suitable nonlinear state estimation and parameter identification techniques for application to the high angle of attack/sideslip flight regime of conventional aircraft have been underway for several years. Dynamics Research Corporation (DRC) has developed a unique proprietary approach to nonlinear state estimation and parameter identification called the Estimation-Before-Modeling (EBM) identification method which determines state-dependent aerodynamic models for the forces and the moments acting on CTOL and V/STOL aircraft in any flight regime. DRC is currently under contract to the Naval Air Development Center to model a conventional aircraft and a V/STOL aircraft using the EBM identification method.

The EBM identification method covers two phases -- state estimation followed by model structure and parameter determination. During the state estimation phase noisy flight records are processed by a unique proprietary DRC estimation approach which uses quadratic spline functions in generating optimal, smoothed time histories of all aircraft states, forces and moments. Various applications of spline functions are given in References [2-12]. Quadratic spline functions are used in DRC's approach to model the unknown time histories of the forces and of the moments. Each quadratic spline function is a function of parameters called knots as well as a function of time. The location of the knots influence the performance of the estimation unless a sufficiently large number of knots are used in the modeling of each force time history and of each moment time history. There is a limit, however, to the practical number of knots that can be used in a computer program. That is, the number of simultaneous equations that must be solved in the estimation process grows at the rate of one parameter per knot per quadratic spline function. Since there are 6 quadratic spline functions - one for each of three forces and one for each of three moments - the number grows at the rate of 6 per knot. For the case of 10 knots per quadratic spline function there is a total of 87 simultaneous equations; the additional 27 simultaneous equations are due to parameters other than those related to knots. The computations and the storage requirement of the estimation process grows exponentially with the number of knots. Consequently, it is advantageous to use as few knots as possible while maintaining an excellent estimation performance. This advantage is realizable by optimally selecting the knot locations. The Optimal Spline Method is an automated technique that performs an optimization of the knot locations and as a result better models of the force and moment time histories are obtained, leading to improved system identification of aircraft.

The Optimal Spline Method is being utilized in a study to develop and apply nonlinear state estimation and parameter identification techniques to high angle of attack/sideslip flight regimes of conventional aircraft and to hover and low-speed flight regimes of V/STOL aircraft. The results [13] of one phase of that study will be presented at the 4th AIAA AFM Meeting in August 8-10, 1977.

CHAPTER II

RESULTS OF AN APPLICATION OF THE OPTIMAL SPLINE METHOD TO SHIP CLASSIFICATION

In Figure 2-1 it is shown how the Optimal Spline Method fits into DRC's approach to ship classification. Note that it is the final block in the feature selection process. Specifically, it extracts the important features of the IRFP stern-bow profile. The IRFP stern-bow profiles are generated by the Image Reconstruction From Projections (IRFP) Method which reconstructs stern-bow images using high range resolution radar data. Before presenting the results of an application of the Optimal Spline Method to ship classification it is necessary to discuss the background of IRFP stern-bow profiles.

A test bed high range resolution radar system having a resolution of 50 feet was used in a Naval Research Laboratory Measurement Program sponsored by the Navy Space Project Office (PME-106) of the Naval Electronic Systems Command to generate profile data of fifteen ship types. Examples of the radar data collected on passes over each of three ship types are shown in the top three plots (1st, 2nd and 3rd projections) of Figures 2-2 through 2-5. The IRFP method which was applied to the top three plots generated the bottom plot called the reconstructed image of the stern-bow profile (i.e., IRFP stern-bow profile). On Run No. 38/Pass No. 8 of the U.S.S. BARNEY the upper three profiles of Figure 2-2 were taken at the aspects (measured clockwise from the ship's bow) 202° , 165° and 135° , respectively. Note the measured radar cross-sections 362, 5540, and 2061 square meters taken at the first, second and third projections, respectively. The projected length of the ship at each projection is noted also. The horizontal axis of each plot denotes the number of range cells (50 feet per range cell) measured from the stern to the bow along the projection. The vertical axis denotes the radar cross-section of the ship's portion contained in the range cell.

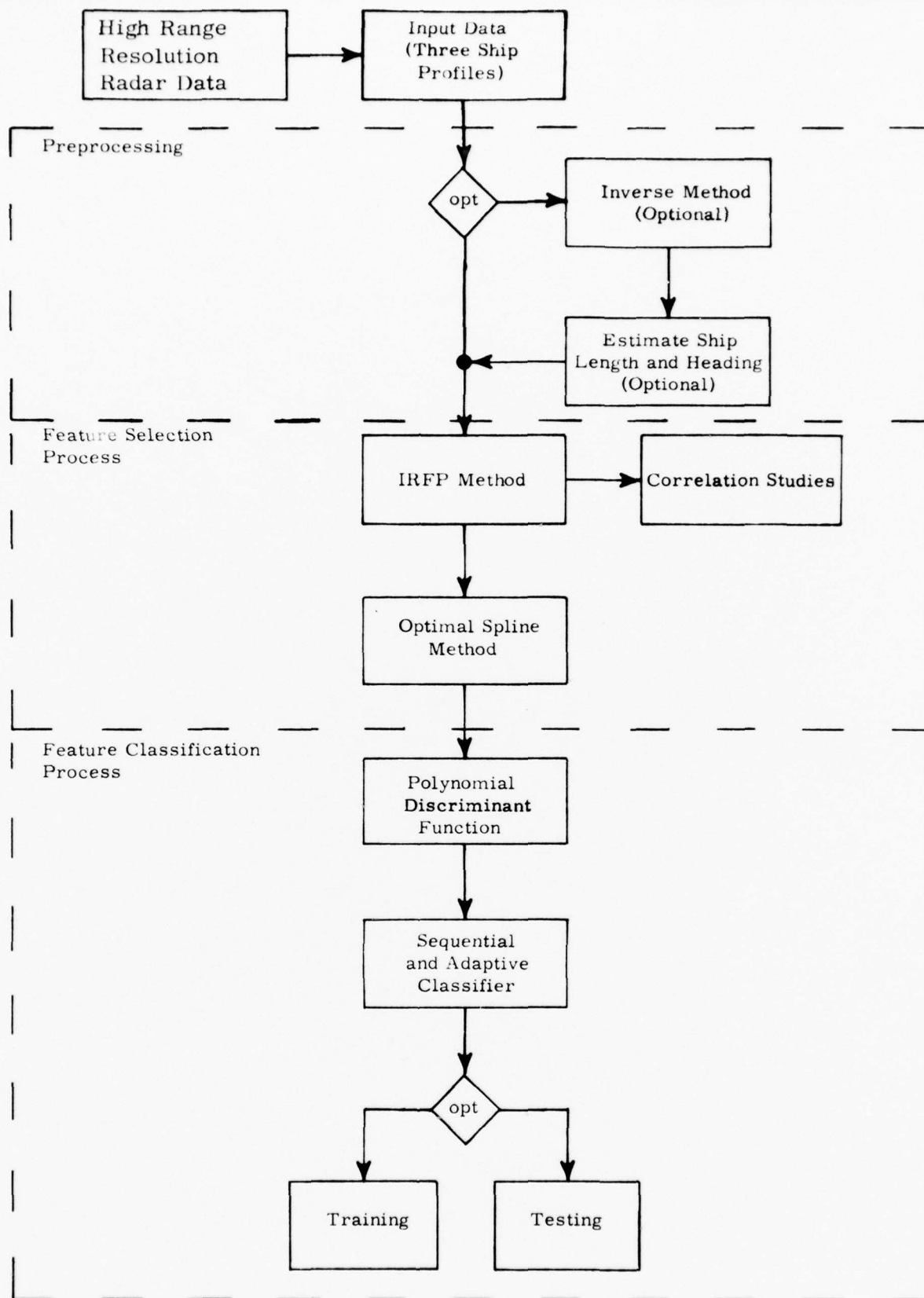
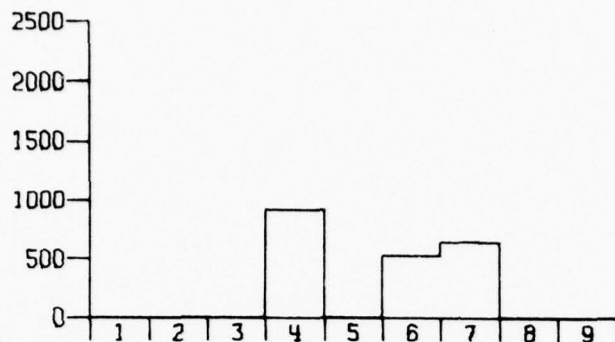


Figure 2-1 Block Diagram of DRC's Ship Classification Approach

1ST PROJECTION

CROSS-SECTION
PER
RANGE CELL
(SQ. M.)



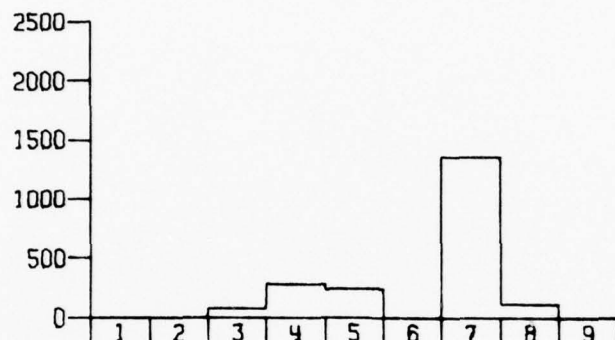
ASPECT ANGLE = 202 DEG.

PROJECTED LENGTH = 413 FEET

CROSS-SECTION = 362 SQ. M.

2ND PROJECTION

(SQ. M.)



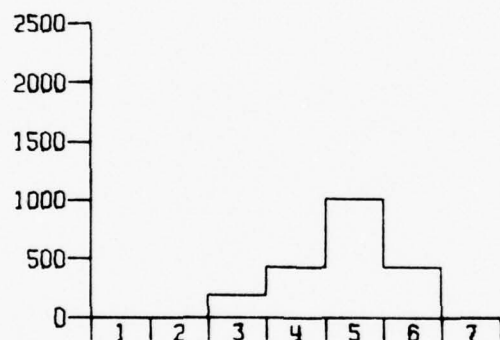
ASPECT ANGLE = 165 DEG.

PROJECTED LENGTH = 425 FEET

CROSS-SECTION = 5540 SQ. M.

3RD PROJECTION

(SQ. M.)



ASPECT ANGLE = 135 DEG.

PROJECTED LENGTH = 333 FEET

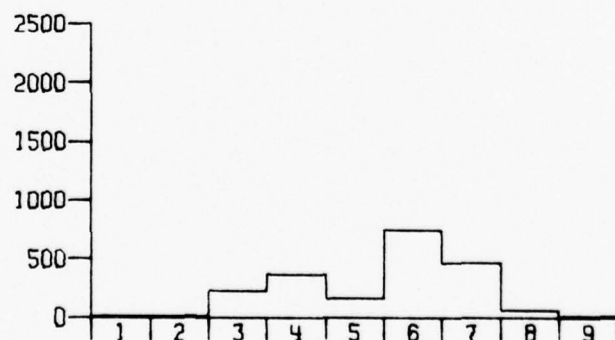
CROSS-SECTION = 2061 SQ. M.

RECONSTRUCTED IMAGE

OF

STERN-BOW
PROFILE

(SQ. M.)



SHIP LENGTH = 437 FEET

SHIP WIDTH = 47 FEET

CROSS-SECTION = 2061 SQ. M.

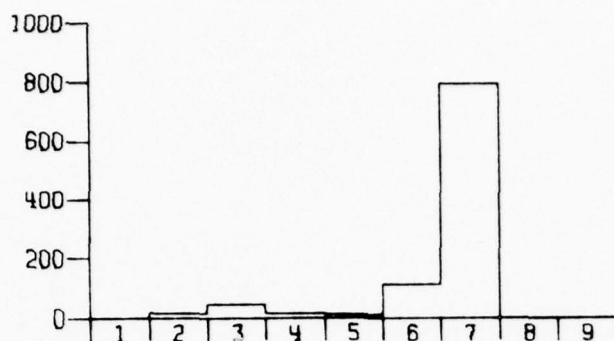
ERROR (LEAST SQUARES) = 8 PERCENT

RANGE CELL (49.7 FEET)

Figure 2-2 IRFP Results of Run No. 38/Pass No. 8 on the U.S.S. BARNEY

1ST PROJECTION

CROSS-SECTION
PER
RANGE CELL
(SQ. M.)



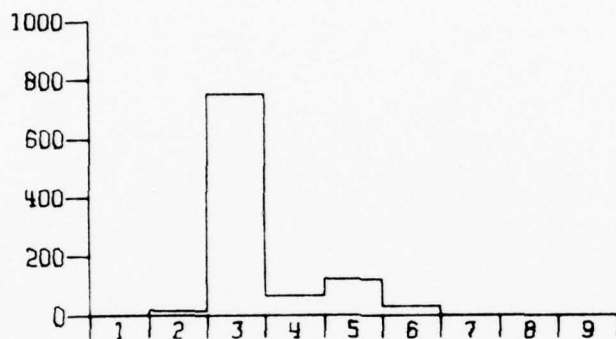
ASPECT ANGLE = 156 DEG.

PROJECTED LENGTH = 406 FEET

CROSS-SECTION = 984 SQ. M.

2ND PROJECTION

(SQ. M.)



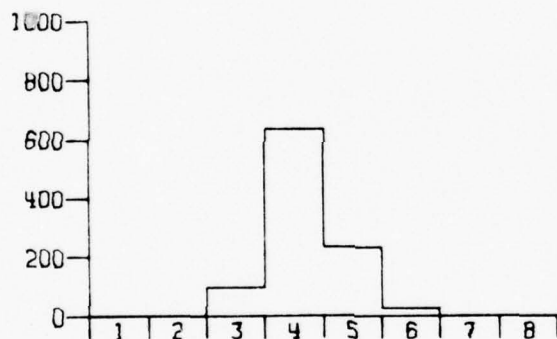
ASPECT ANGLE = 189 DEG.

PROJECTED LENGTH = 433 FEET

CROSS-SECTION = 293 SQ. M.

3RD PROJECTION

(SQ. M.)



ASPECT ANGLE = 219 DEG.

PROJECTED LENGTH = 359 FEET

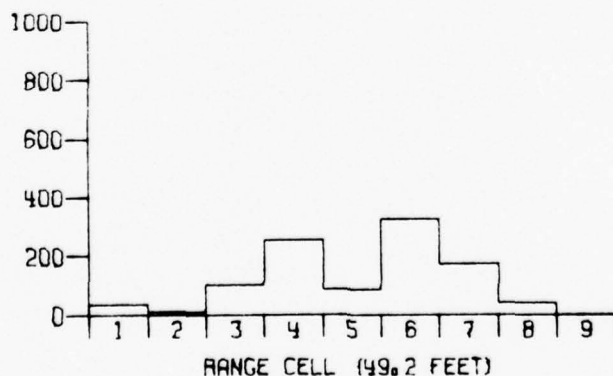
CROSS-SECTION = 2264 SQ. M.

RECONSTRUCTED IMAGE

OF

STERN-BOW
PROFILE

(SQ. M.)



RANGE CELL (49.2 FEET)

SHIP LENGTH = 437 FEET

SHIP WIDTH = 47 FEET

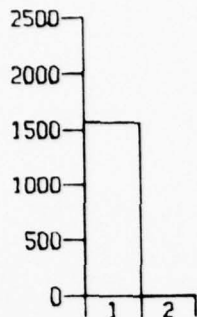
CROSS-SECTION = 984 SQ. M.

ERROR (LEAST SQUARES) = 20 PERCENT

Figure 2-3 IRFP Results of Run No. 40/Pass No. 6 on the U.S.S. BARNEY

1ST PROJECTION

CROSS-SECTION
PER
RANGE CELL
(SQ. M.)



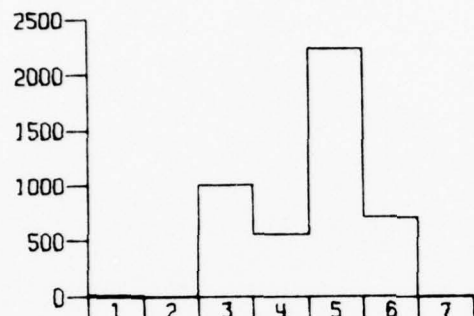
ASPECT ANGLE = 92 DEG.

PROJECTED LENGTH = 66 FEET

CROSS-SECTION = 51280 SQ. M.

2ND PROJECTION

(SQ. M.)



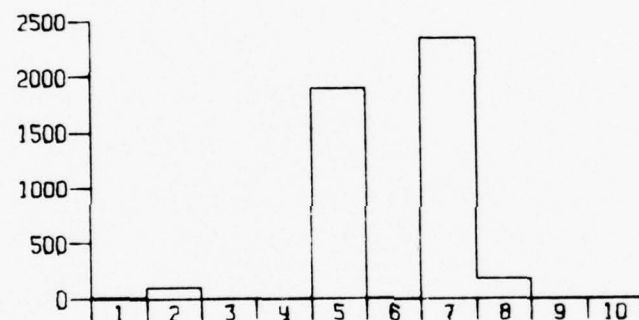
ASPECT ANGLE = 125 DEG.

PROJECTED LENGTH = 332 FEET

CROSS-SECTION = 3583 SQ. M.

3RD PROJECTION

(SQ. M.)



ASPECT ANGLE = 159 DEG.

PROJECTED LENGTH = 486 FEET

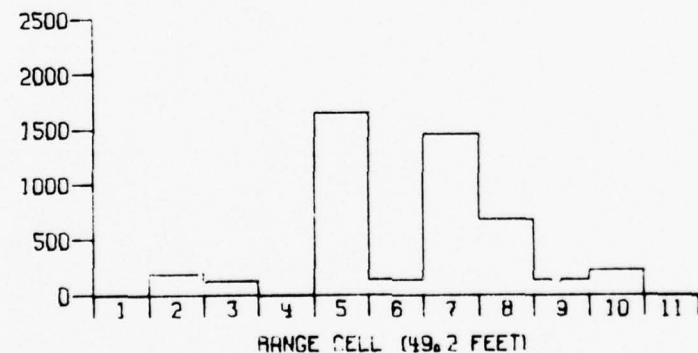
CROSS-SECTION = 4513 SQ. M.

RECONSTRUCTED IMAGE

OF

STERN-BOW
PROFILE

(SQ. M.)



SHIP LENGTH = 513 FEET

SHIP WIDTH = 53 FEET

CROSS-SECTION = 4513 SQ. M.

ERROR (LEAST SQUARES) = 13 PERCENT

RANGE CELL (49.2 FEET)

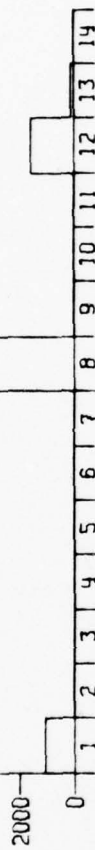
Figure 2-4 IRFP Results of Run No. 32/Pass No. 1 on the U.S.S. DAHLGREN

RUN NO. 44 / PASS NO. 1

1ST PROJECTION

CROSS-SECTION
PEL
RANGE CELL
(SQ. M.)

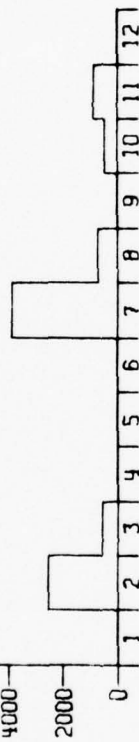
ASPECT ANGLE = 176 DEG.
PROJECTED LENGTH = 676 FEET
CROSS-SECTION = 8912 SQ. M.



2ND PROJECTION

(SQ. M.)

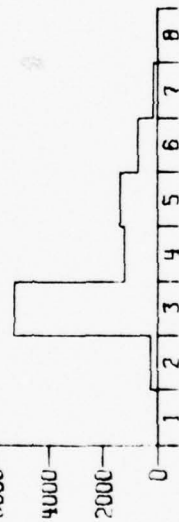
ASPECT ANGLE = 218 DEG.
PROJECTED LENGTH = 568 FEET
CROSS-SECTION = 10072 SQ. M.



3RD PROJECTION

(SQ. M.)

ASPECT ANGLE = 245 DEG.
PROJECTED LENGTH = 360 FEET
CROSS-SECTION = 3961 SQ. M.



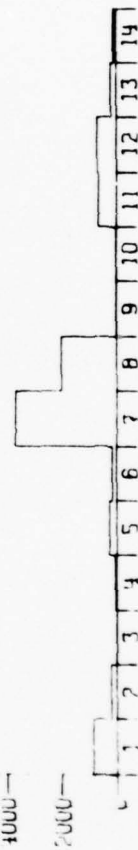
RECONSTRUCTED
IMAGE

OF

STEIN-BOW
PHOTO

(SQ. M.)

SHIP LENGTH = 677 FEET
SHIP WIDTH = 84 FEET
CROSS-SECTION = 8912 SQ. M.
ERROR (LEAST SQUARES) = 9 PERCENT



RANGE CELL (49.2 FEET)

Figure 2-5 IRFP Results of Run No. 44/Pass No. 1 on the ESSO DENMARK Tanker

The bottom profile is the output of the IRFP method resulting from the input of the upper three profiles. This is the reconstructed image of the U.S.S. BARNEY. The left end of the profile represents the stern and the right end the bow. The IRFP results of another pass over the U.S.S. BARNEY are given in Figure 2-3. A broadside drawing of the U.S.S. BARNEY (DDG-6) is given in Figure 2-6. Note the similarity between the IRFP stern-bow profiles of Figures 2-2 and 2-3 and the superstructure of the U.S.S. BARNEY in Figure 2-6. The IRFP results of a pass over the U.S.S. Dahlgren and of a pass over a Danish tanker (the ESSO DENMARK) are given in Figures 2-4 and 2-5, respectively. A drawing of the U.S.S. DAHLGREN is presented in Figure 2-7. A picture of the ESSO DENMARK is shown in Figure 2-8. In all passes the upper three profiles have been normalized to a total cross-section of the projection that lies between the cross-section of the other two projections. The IRFP profile has been normalized to this same cross-section.

The results of the application of the Optimal Spline Method to the IRFP stern-bow profiles of Run 38/Pass 8, Run 40/Pass 6, Run 32/Pass 1 and Run 44/Pass 1 are contained in Figures 2-9 through 2-12, respectively. In this application the radar cross-section is normalized to unity. The coefficient of the optimal spline function for each spline region is symbolized by the notation "PBAR". Optimally placed knots are denoted by the notation "OPTIMAL". For example, in Figure 2-9 the value of \ddot{r}_1 , (i.e., the first component of the p vector Equation(4.16)) for the first spline region $[0.0, 0.72]$ is equal to 0.19; the first knot is optimally located at 0.72. The second knot is optimally placed at 2.75. Since each range cell represents 50 feet along the ship's length and since the stern starts at zero it follows that the first knot falls at 0.72×50 feet = 36 feet from the stern, the second at 138 feet, etc.

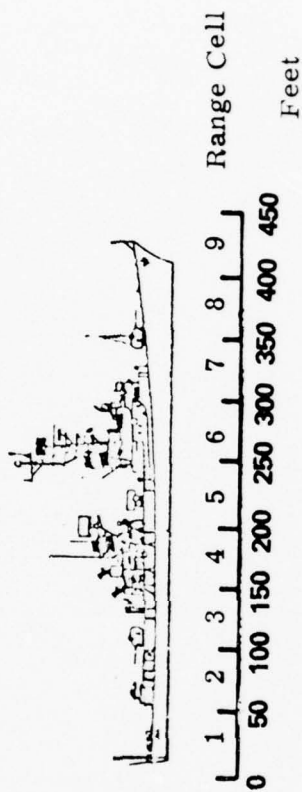


Figure 2-6. Broadside Drawing of the U. S. S. BARNEY (DDG-6)

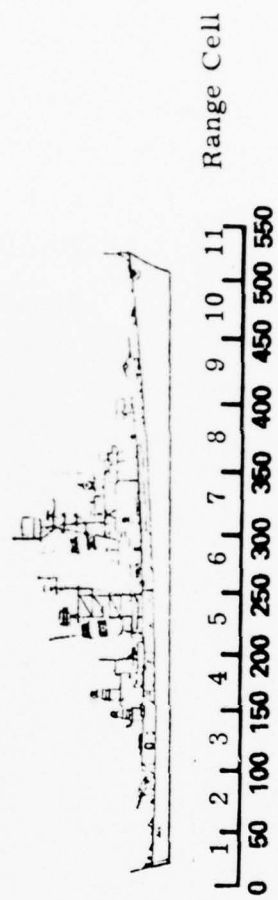


Figure 2-7. Broadside Drawing of the U. S. S. DAHLGREN (DLG-12)

Range cells measured from stern

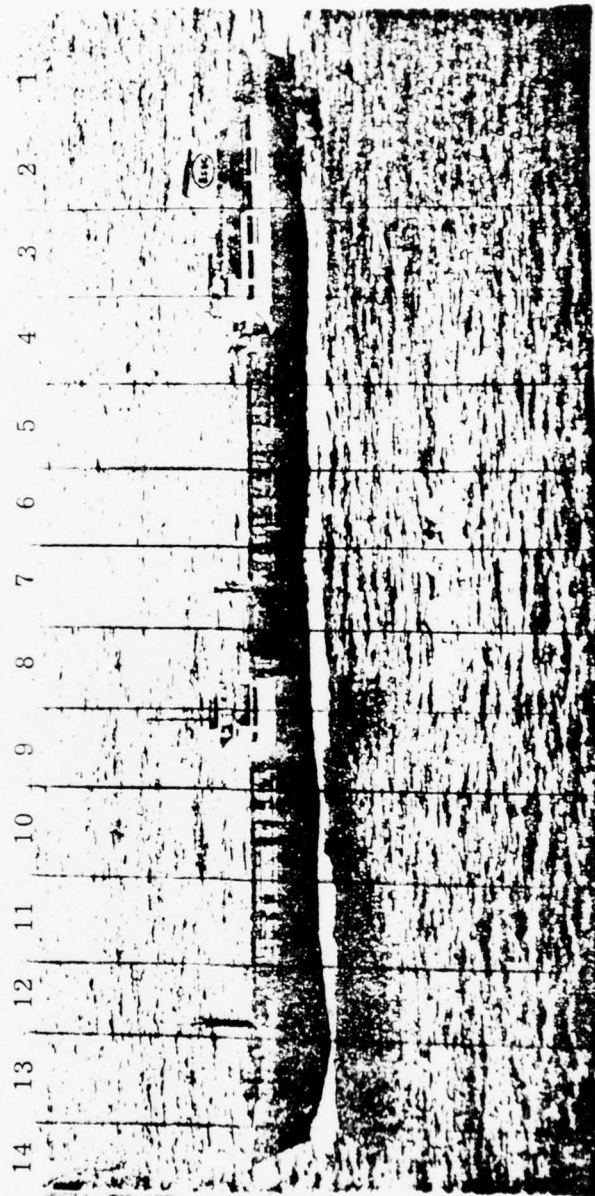


Figure 2-8. ESO DENMARK Tanker, Length = 677 feet, 49.2 ft. Divisions

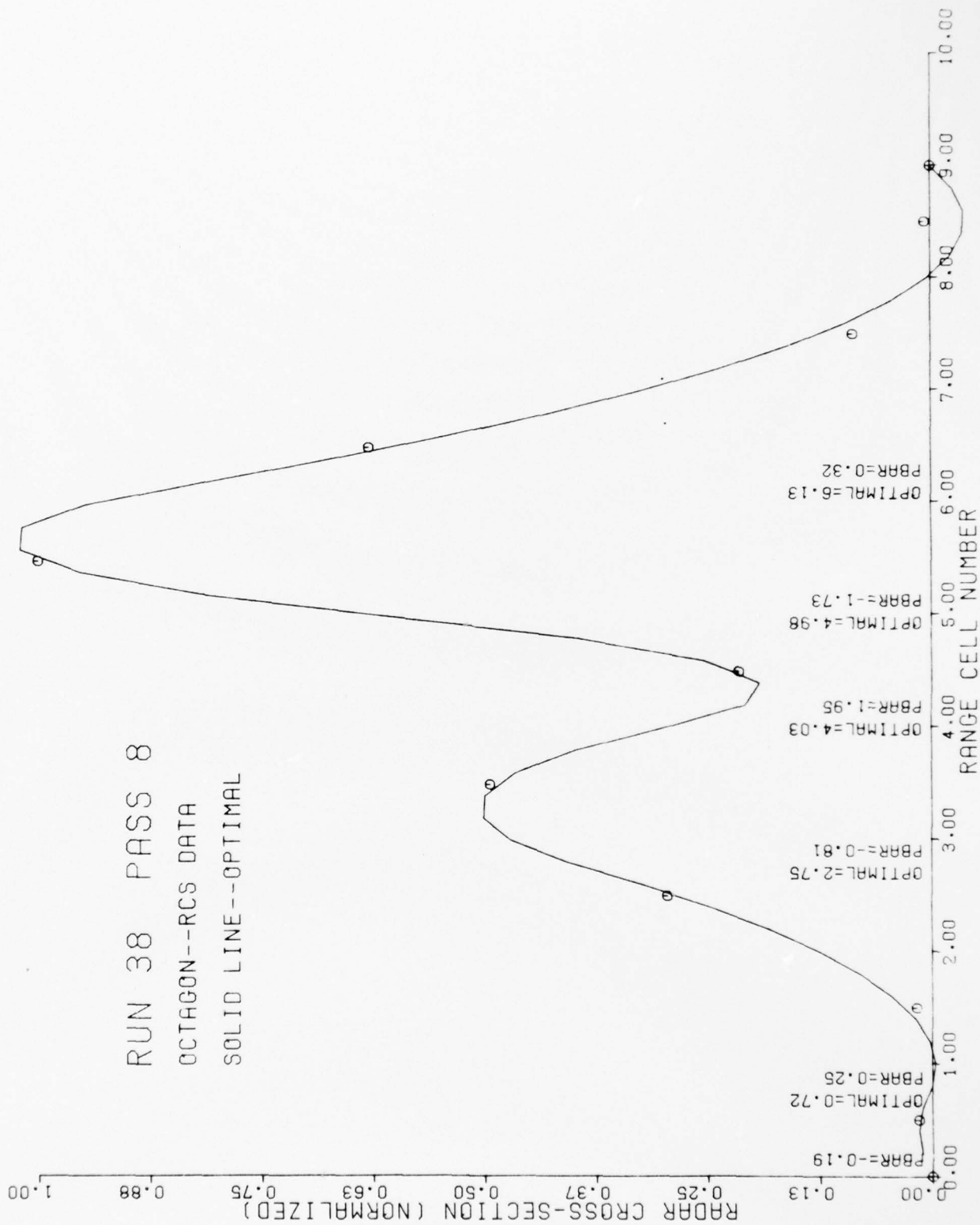


Figure 2-9. Optimal Spline Method Results of Run No. 38/Pass No. 8

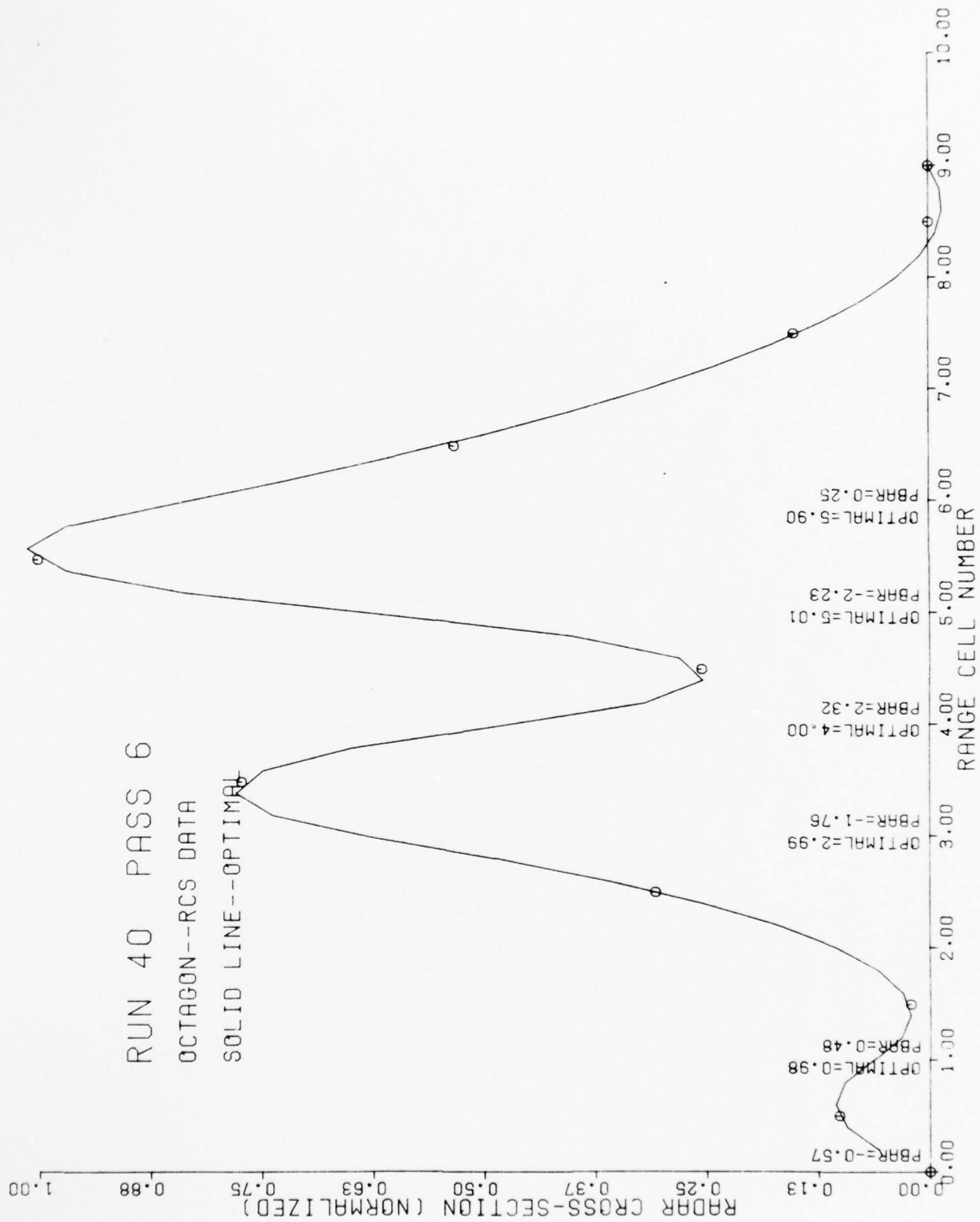


Figure 2-10. Optimal Spline Method Results of Run No. 40 / Pass No. 6

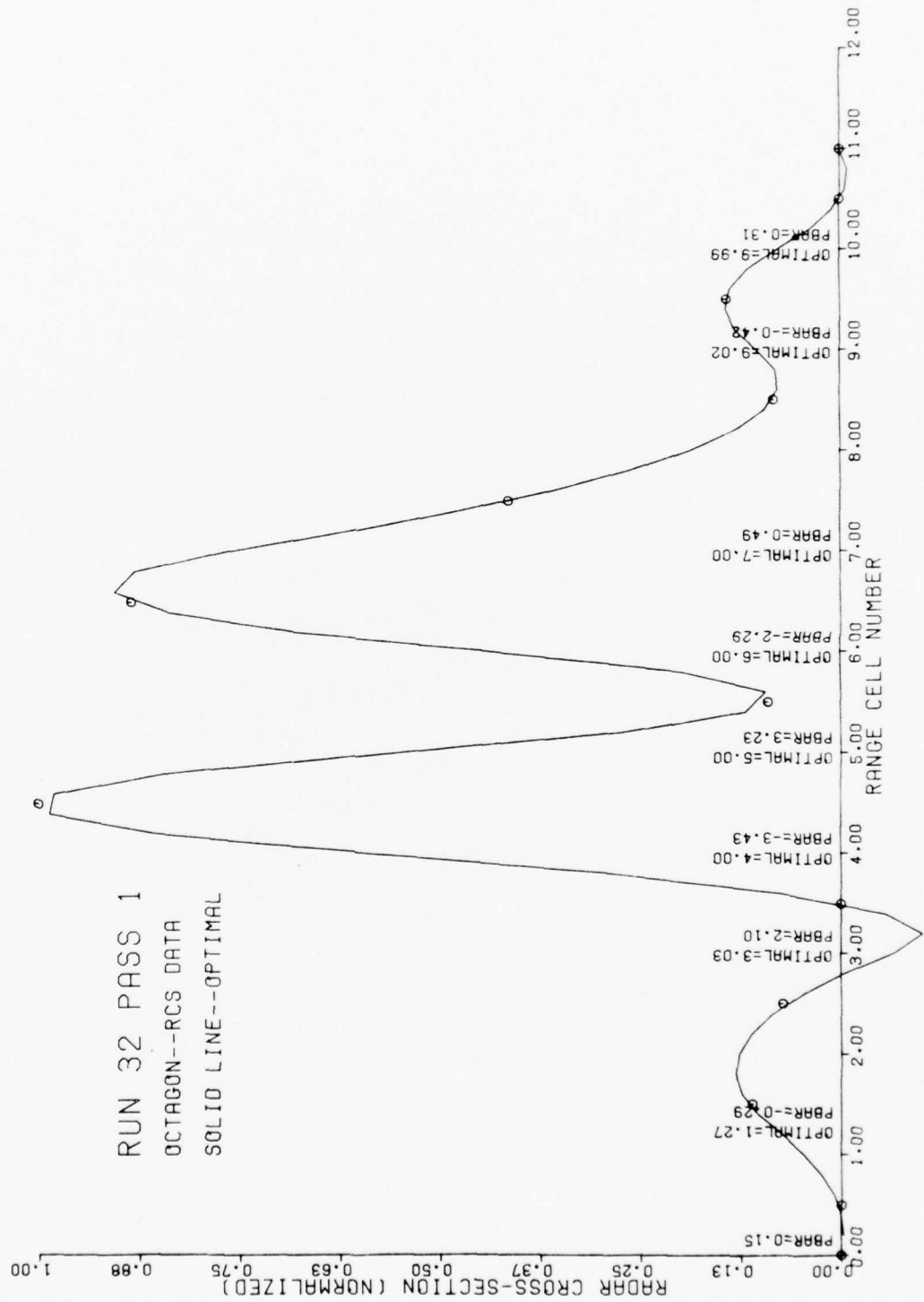


Figure 2-11. Optimal Spline Method Results of Run No. 32/Pass No. 1

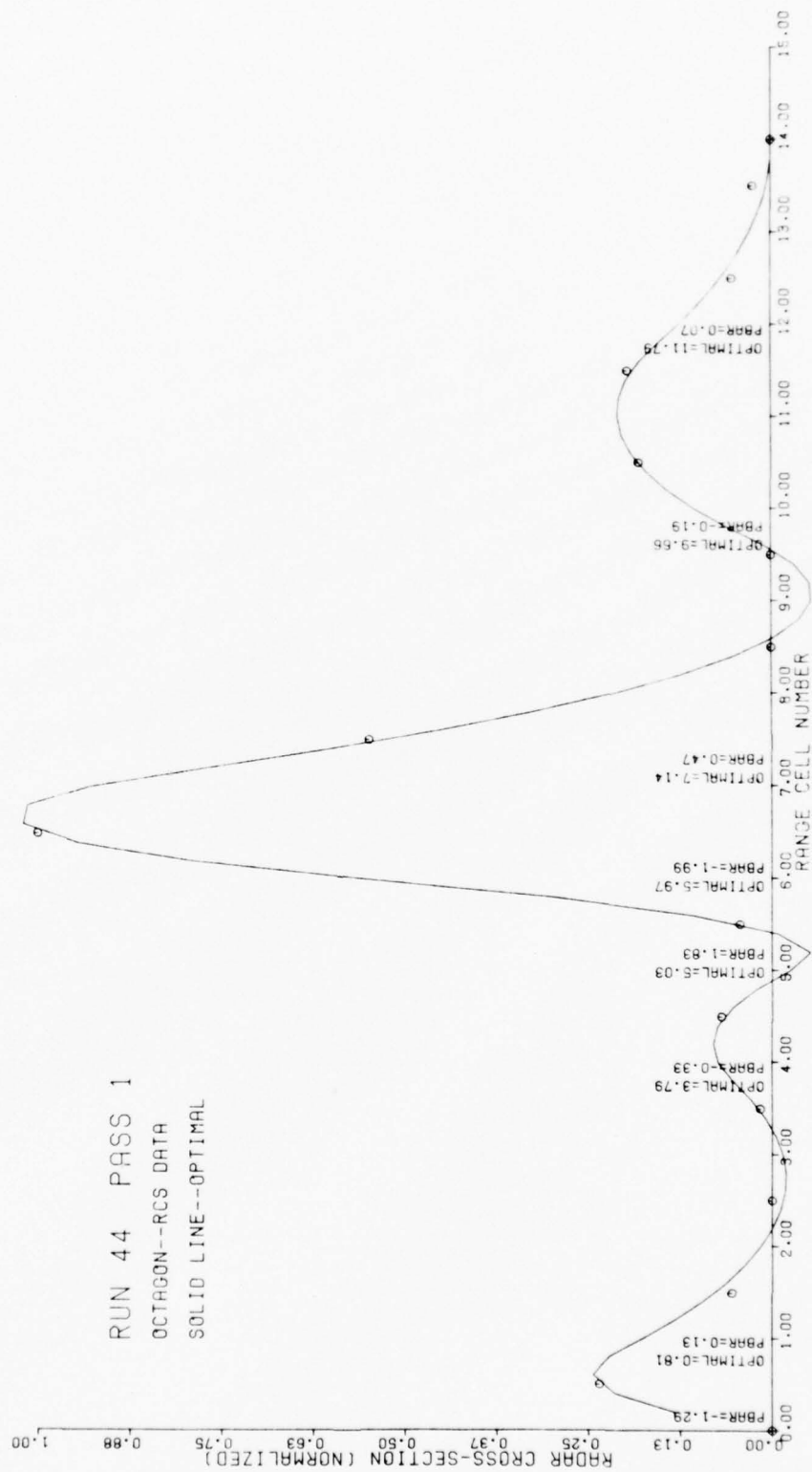


Figure 2-12. Optimal Spline Results of Run No. 44/Pass No. 1

The number of knots, an output of the Optimal Spline Method, is five for both U.S.S. BARNEY passes - Figures 2-9 and 2-10. Note that eight knots were calculated for the U.S.S. DAHLGREN and seven for the ESSO DENMARK - Figures 2-11 and 2-12, respectively. The knot locations and the optimal spline coefficient values are tabulated in Tables 2-1 and 2-2.

Analyzing the first two columns of Table 2-1 and the first two columns of Table 2-2 we see that for both U.S.S. BARNEY passes the knot locations and the coefficient values are in good agreement. Looking at the third column of Table 2-2 we observe that the coefficients for the U.S.S. DAHLGREN differ from those of the U.S.S. BARNEY in sign as well as in magnitude. These differences together with the difference of 5 knots for the U.S.S. BARNEY versus 8 knots for the U.S.S. DAHLGREN make it easy to distinguish these two ship types.

It is also easy to distinguish between the ESSO DENMARK and the U.S.S. BARNEY because (1) there are five knots for the U.S.S. BARNEY and seven for the ESSO DENMARK, (2) their knot locations differ considerably and (3) their optimal spline coefficients differ greatly in magnitude for some of the spline regions.

Furthermore, it is easy to distinguish between the ESSO DENMARK and the U.S.S. DAHLGREN because (1) their coefficients differ in sign and (2) they have differences in knot locations.

Optimally locating the knots has two advantages. The first is the extraction of the independent features for classification purposes. The second is the reduction of the least-squares error. In Table 2-3 is presented a comparison of the least-squares error between optimally located knots and equally spaced knots. The least-squares error of Run No. 38/

Table 2-1
Comparison of Optimal Spline Knot Locations

Knot Index	Location of ith Knot			
	U.S.S. BARNEY Run 38/Pass 8	U.S.S. BARNEY Run 40/Pass 6	U.S.S. DAHLGREN Run 32/Pass 1	ESSO DENMARK Run 44/Pass 1
1	.72	.98	1.27	.81
2	2.75	2.99	3.03	3.79
3	4.03	4.00	4.00	5.03
4	4.98	5.01	5.00	5.97
5	6.13	5.90	6.00	7.14
6	-	-	7.00	9.66
7	-	-	9.02	11.79
8	-	-	9.99	-

Table 2-2

Comparison of Optimal Spline Coefficient Values

Spline Region Index	Value of Optimal Spline Coefficient of i th Spline Region			
	U.S.S. BARNEY Run 38/Pass 8	U.S.S. BARNEY Run 40/Pass 6	U.S.S. DAHLGREN Run 32/Pass 1	ESSO DENMARK Run 44/Pass 1
1	-.19	-.57	.15	-1.29
2	.25	.48	-.29	.13
3	-.81	-1.76	2.10	-.33
4	1.95	2.32	-3.43	1.83
5	-1.73	-2.23	3.23	-1.99
6	.32	.25	-2.29	.47
7	-	-	.49	-.19
8	-	-	-.42	.07
9	-	-	.31	-

Table 2-3

Comparison of Least-Squares Error Between Optimally Located
Knots and Equally Spaced Knots

Run No./Pass No.	Number of Knots	Least-Squares Error	
		Optimally Located Knots	Equally Spaced Knots
U.S.S. BARNEY 38/8	5	.01	.87
U.S.S. BARNEY 40/6	5	.08	1.23
U.S.S. DAHLGREN 32/1	8	.004	.44
ESSO DENMARK 44/1	7	.06	1.45

Pass No. 8 for optimally located knots is .01 and the error of the same run for equally spaced knots is .87. The ratio of the error associated with equally spaced knots to the error associated with optimally located knots is 87. In all cases this ratio is greater than 10.

CHAPTER III

RESULTS OF AN APPLICATION OF THE OPTIMAL SPLINE METHOD TO AIRCRAFT SYSTEM IDENTIFICATION

Aerodynamic derivatives are highly dependent on the angle of attack variable α and the sideslip angle variable β . Thus, these angles are important state variables in the state-dependent modeling of the forces and the moments that act on an aircraft. Presented in Figures 3-1 and 3-2 are applications of the Optimal Spline Method to angle of attack and sideslip angle flight test data of a light jet trainer aircraft. The Optimal Spline Method calculated twelve knots for the angle of attack data and optimally located them as shown in Figure 3-1. It calculated eight for the sideslip angle and optimally located them as shown in Figure 3-2. The first knot denoted by "OPTIMAL" for the sideslip angle is optimally placed at 4.62 seconds; the spline coefficient which is denoted by "PBAR" is 0.02 for the first spline region, 0.30 for the second spline region, etc.

Equally spaced knots have been used to fit the same angle of attack and sideslip angle data. The result of using twelve equally spaced knots on the angle of attack data is shown in Figure 3-3. The fit is not adequate at the times 3.5, 5.5, 7.5, 9.3, 10.7, 13.7, and 14.7. At each of these times the smooth curve falls outside the statistical limits of the noise. Shown in Figure 3-4 is the result of the use of eight equally spaced knots for the sideslip data. An unsatisfactory fit is even more pronounced here than it is in Figure 3-3. Consequently, equally spaced knots provide unsatisfactory smoothing unless an abundance of them are used. The Optimal Spline Method provides an adequate fit with a reduced number of knots by optimally locating them so that the resulting smooth curve can stay in phase with the data.

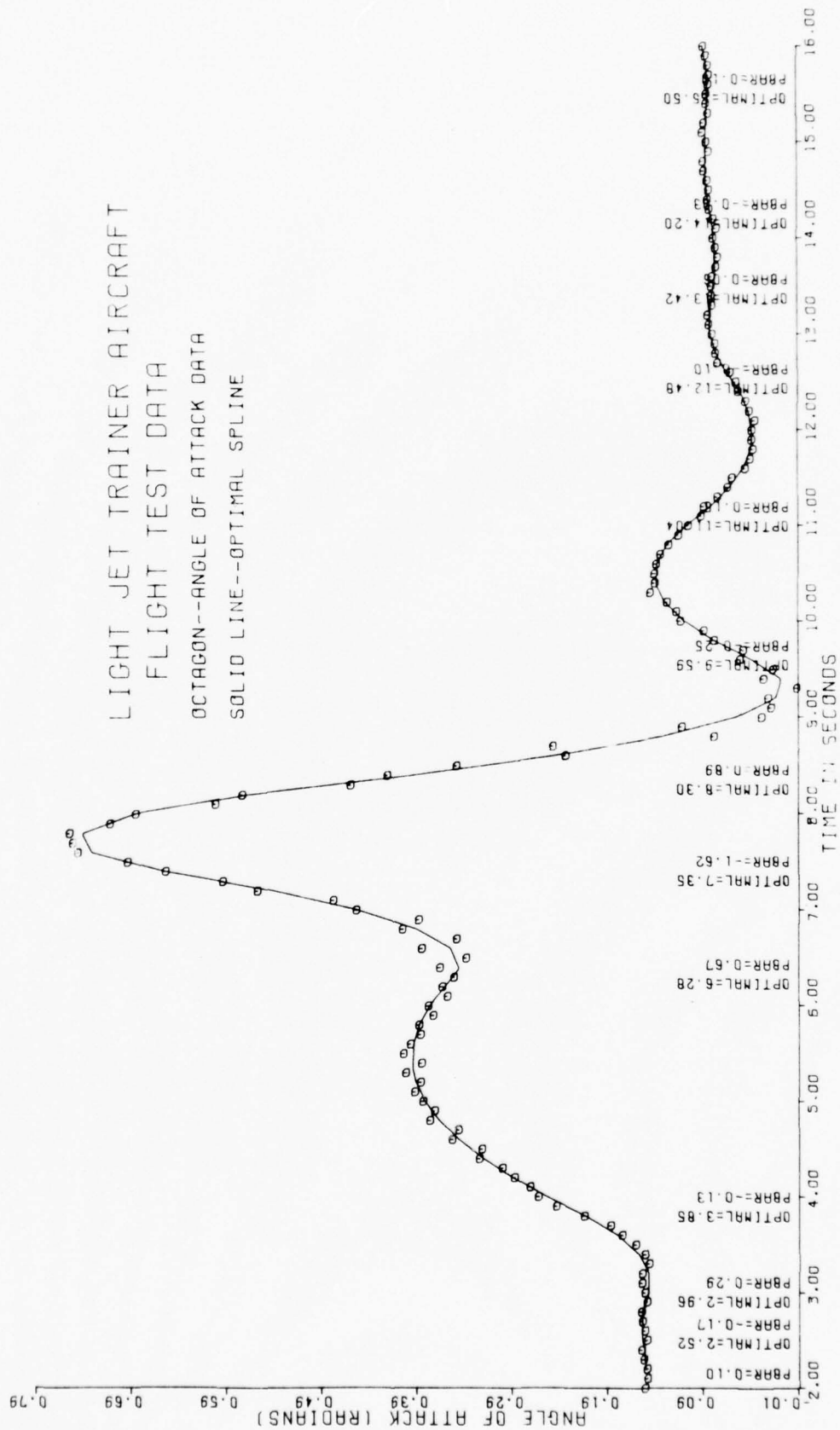


Figure 3-1. Optimal Spline Method Application to Angle of Attack Data

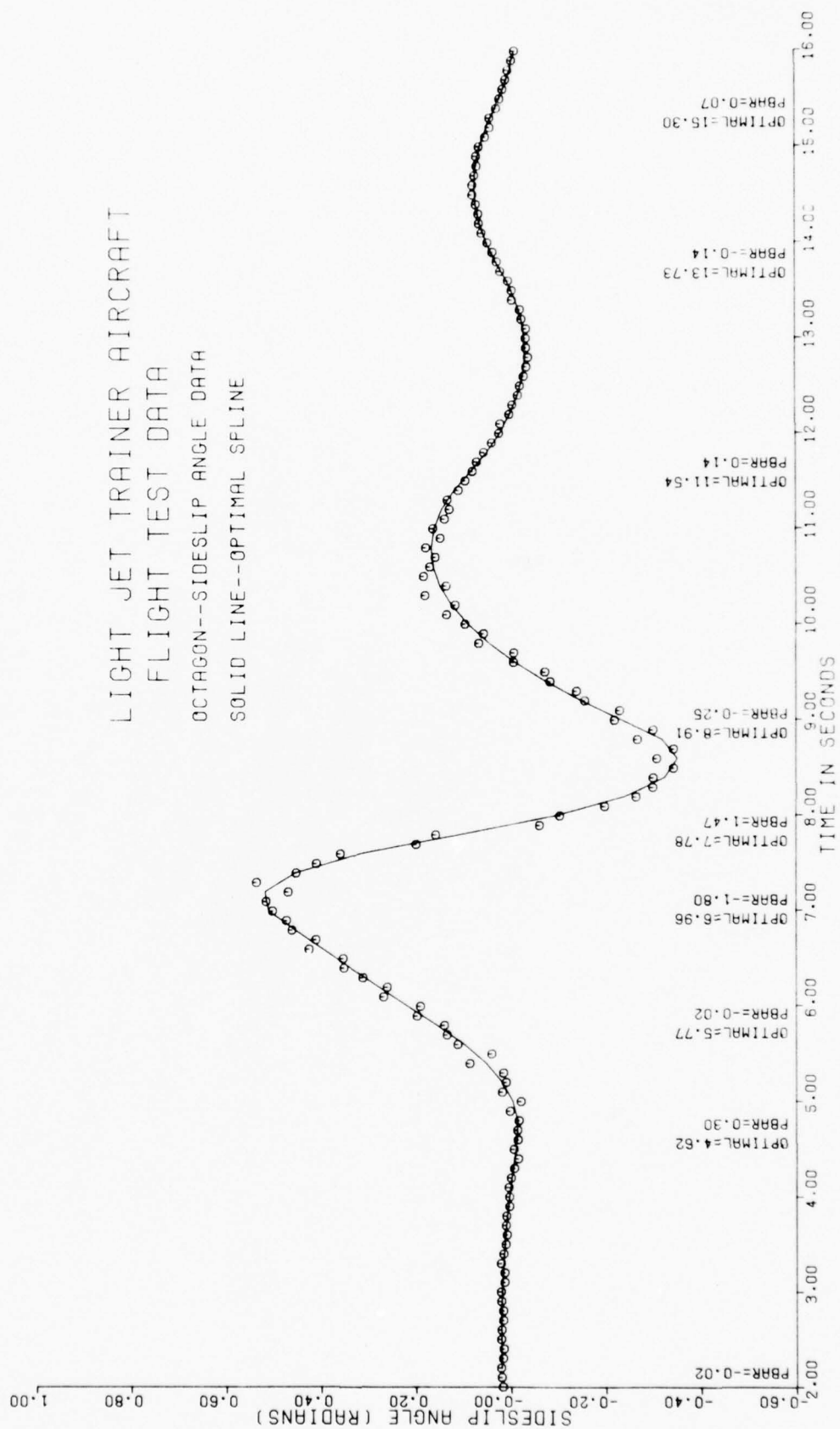


Figure 3-2. Optimal Spline Method Application to Sideslip Angle Data

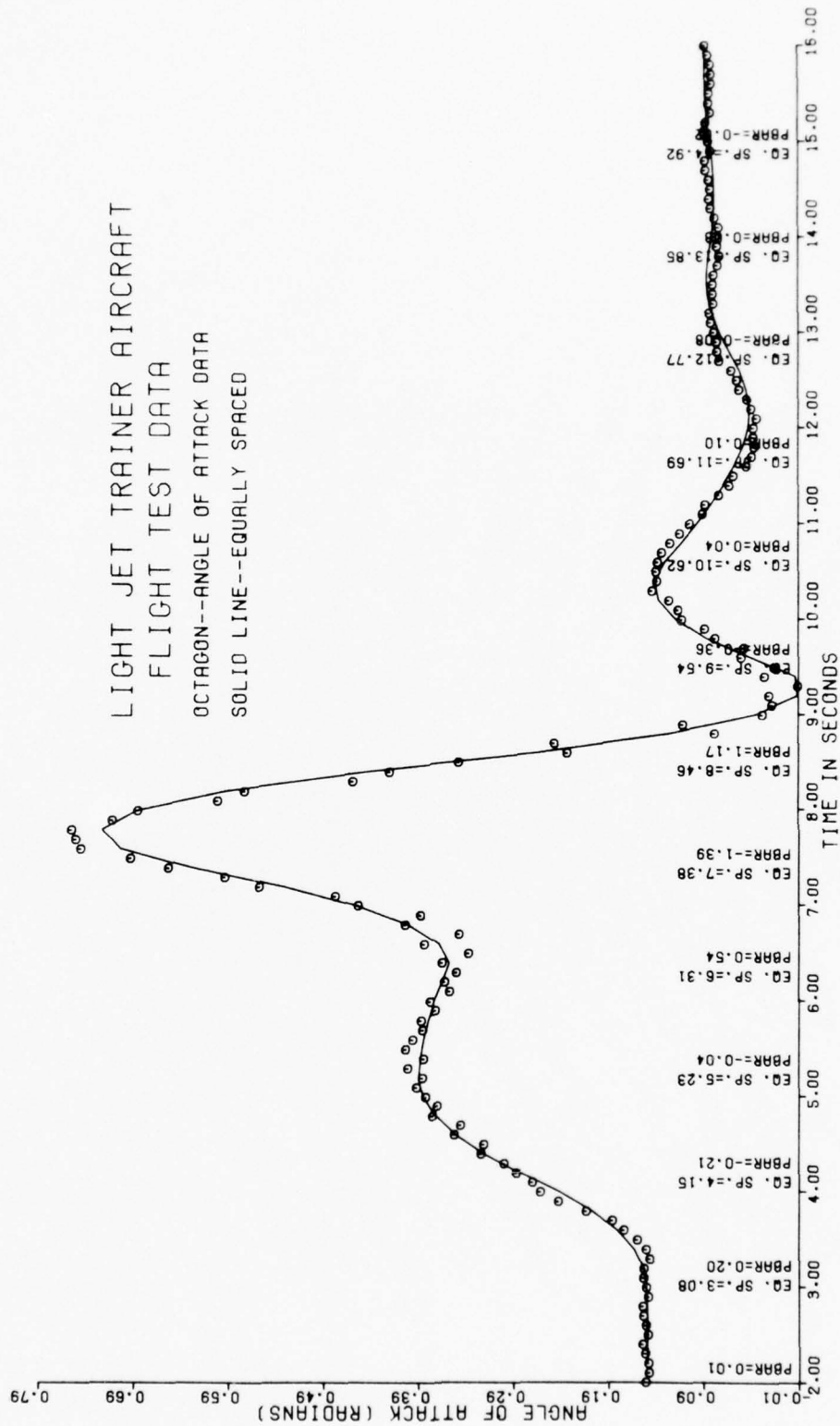


Figure 3-3. Equally Spaced Knots Results of Angle of Attack Data

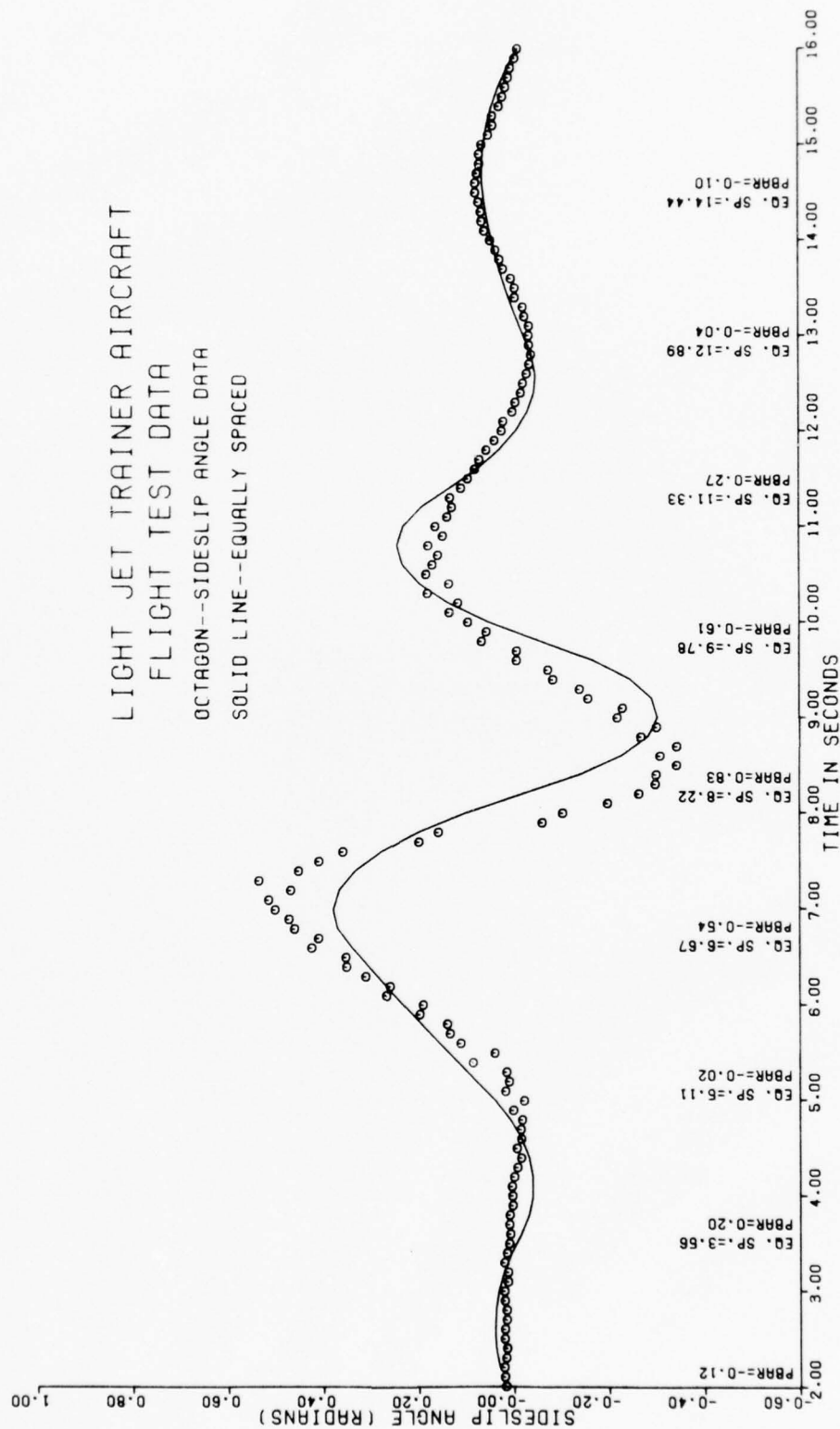


Figure 3-4. Equally Spaced Knots Results of Sideslip Angle Data

CHAPTER IV

MATHEMATICAL DESCRIPTION OF PROBLEM

4.1 Time Function Representations

The problem being investigated deals with the representation of a time function by the superposition of a family of simple functions which are easy to define, generate and implement. In particular, it is sought to minimize the number of parameters in such representations, while maintaining a required degree of accuracy.

Let $f(t)$ denote a square integrable time function defined over a time interval $[T_o, T_f]$. Let $d(t)$ be a measured time history of $f(t)$:

$$d(t) = f(t) + \eta \quad (4.1)$$

where η is a stationary Gaussian process with variance σ^2 .

Let $\{ \alpha_n(t): n = 1, 2, \dots \}$ denote the family of simple square integrable functions to be used in the superposition. Since only a finite number of terms, N , is possible for a practical realization of $f(t)$, it is necessary to choose coefficients q_1, q_2, \dots, q_N so as to render a minimum to the criterion:

$$E = \int_{T_o}^{T_f} \left[d(t) - \sum_{n=1}^N q_n \alpha_n(t) \right]^2 dt \quad (4.2)$$

For the case of a complete orthonormal function series (e.g., Fourier, Walsh, Haar) the minimum is attained by making

$$q_n = \int_{T_0}^{T_f} d(t) \alpha_n(t) dt \quad (4.3)$$

and the error E monotonically decreases to the variance σ^2 as N becomes very large.

The advantage of using orthogonal series is the ease with which the optimum q_n 's of (4.2) are computable, i.e., using Equation (4.3). Frequently, a large value of N is needed in order that the error E is sufficiently close to σ^2 . Large values of N are disadvantageous in some applications (e.g., ship classification and aircraft system identification). There are nonorthogonal function series that provide excellent fits and use only small values of N .

One such nonorthogonal series is composed of quadratic spline functions. Before introducing these functions the solution of (4.2) will be derived for nonorthogonal series. Define† the row vector \underline{q}^T as

$$\underline{q}^T = (q_1, q_2, \dots, q_n) \quad (4.4)$$

the row vector $\underline{\alpha}^T(t)$ as

$$\underline{\alpha}^T(t) = (\alpha_1(t), \alpha_2(t), \dots, \alpha_n(t)) \quad (4.5)$$

†The superscript T denotes transpose.

and the matrix B whose i^{th} row and j^{th} column element b_{ij} is given by

$$b_{ij} = \int_{T_0}^{T_f} \alpha_i(t) \alpha_j(t) dt \quad (4.6)$$

The solution of (4.2) is given by

$$\underline{q} = B^{-1} \int_{T_0}^{T_f} d(t) \underline{\alpha}(t) dt \quad (4.7)$$

For the case that B is the identity matrix this solution reduces to (4.3).

4.2 QUADRATIC SPLINE FUNCTIONS

Consider the following general 2nd order nonlinear differential equation

$$\ddot{r}(t) = f(t, r(t), \dot{r}(t)) \quad (4.8)$$

where r and f are scalars and where f is a continuously differentiable function. Integrating both sides of this equation twice with respect to time over the interval $[T_0, t]$ gives

$$r(t) = \dot{r}(T_0) + r(T_0)(t - T_0) + \int_{T_0}^t \int_{T_0}^{\tau} f(s, r(s), \dot{r}(s)) ds d\tau \quad (4.9)$$

The double integral can be rewritten as

$$\int_{T_0}^t \int_{T_0}^{\tau} \delta(s, \tau) f(s, r(s), \dot{r}(s)) ds d\tau$$

where

$$\delta(s, \tau) = \begin{cases} 1 & s \leq \tau \\ 0 & s > \tau \end{cases} \quad (4.10)$$

Interchanging the order of integration and carrying out the integration results in

$$\int_{T_0}^t (t-s) f(s, r(s), \dot{r}(s)) ds$$

Consequently $r(t)$ can be rewritten as

$$r(t) = r_0 + \dot{r}_0 (t - T_0) + \int_{T_0}^t (t-s) f(s, r(s), \dot{r}(s)) ds \quad (4.11)$$

where $r_0 \triangleq r(T_0)$ and $\dot{r}_0 \triangleq \dot{r}(T_0)$. This equation is the integral equivalent of the differential equation. The integral term is evaluated as follows: The total time domain of interest $[T_0, T_f]$ is divided into a number of subregions $[T_{j-1}, T_j]$, $j = 1, 2, \dots, m+1$ called "splines". The points T_1, T_2, \dots, T_m are called knots. Here, $T_{m+1} = T_f$. The integral can be written equivalently as a sum of integrals over each spline region, i.e.,

$$r(t) = r_0 + \dot{r}_0 (t - T_0) + \sum_{k=1}^{j-1} \int_{T_{k-1}}^{T_k} (t-s) f(s, r(s), \dot{r}(s)) ds + \int_{T_{j-1}}^t (t-s) f(s, r(s), \dot{r}(s)) ds \quad (4.12)$$

where $t \in [T_{j-1}, T_j]$, $j = 1, 2, \dots, m+1$. By choosing sufficiently many splines we can model $f(s, r(s), \dot{r}(s))$ as a constant \ddot{r}_j over each spline region $[T_{j-1}, T_j]$, $j = 1, 2, \dots, m+1$. With this approximation $r(t)$ becomes

$$r(t) = r_0 + \dot{r}_0 (t - T_0) + \sum_{k=1}^{j-1} (T_k - T_{k-1}) \left(t - \frac{T_{k-1} + T_k}{2} \right) \ddot{r}_k + \frac{(t - T_{j-1})^2}{2} \ddot{r}_j \quad (4.13)$$

where $t \in [T_{j-1}, T_j]$. This is the quadratic spline function. The family of such functions is generated by letting the knots and the parameters $r_0, \dot{r}_0, \ddot{r}_1, \dots, \ddot{r}_m$ vary over their regions of definition. In vector form the quadratic spline function can be written as

$$\underline{r}(t) = \underline{a}^T(t; \underline{T}) \cdot \underline{p} \quad (4.14)$$

where the knot vector \underline{T} is given by

$$\underline{T} = (T_1, T_2, \dots, T_m), \quad (4.15)$$

where

$$\underline{p} = (\ddot{r}_1, \dots, \ddot{r}_{m+1}, r_0, \dot{r}_0) \quad (4.16)$$

$$\underline{a}^T(t; \underline{T}) = (a_1(t; \underline{T}), a_2(t; \underline{T}), \dots, a_{m+3}(t; \underline{T})) \quad (4.17)$$

$$a_{m+2}(t; \underline{T}) = 1 \quad (4.18)$$

$$a_{m+3}(t; \underline{T}) = t - T_0 \quad (4.19)$$

and where, for $j = 1, 2, \dots, m+1$,

$$a_j(t; \underline{T}) = \begin{cases} 0 & T_0 \leq t \leq T_{j-1} \\ \frac{(t - T_{j-1})^2}{2} & T_{j-1} \leq t \leq T_j \\ (T_j - T_{j-1}) \left(t - \frac{T_{j-1} + T_j}{2} \right) & t \geq T_j \end{cases} \quad (4.20)$$

In an application to ship classification the function r represents the radar cross-section per unit range resolution (i.e., density) along the length of the ship from the stern to the bow. Since this density is zero at the beginning of the stern and at the end of the bow the constraints

$$r_0 = 0 \quad (4.21)$$

$$r(T_{m+1}) = 0 \quad (4.22)$$

must necessarily be invoked. The coefficients r_j , $j = 1, 2, \dots, m+1$ provide a composite picture of the ship's superstructure.

To put the quadratic spline function in the notation of Section 4.1 let the vector \underline{T} be fixed and define

$$\alpha_j(t) = a_j(t; \underline{T}) \quad j = 1, 2, \dots, N \quad (4.23)$$

where $N = m+3$. The vector \underline{q} corresponds to the vector \underline{p} .

4.3 A GENERAL TIME FUNCTION OPTIMIZATION PROBLEM

The quadratic spline functions introduced in the previous subsections provide a family of simple functions for the representation of a time function. The quadratic spline functions form a nonorthogonal function series that quadratically depend on a parameter set \underline{T} of knots. In general, then, a family of simple functions for time function representation will depend on a set of parameters such as \underline{T} and the dependence will be possibly nonlinear. Consequently a general time function

optimization problem has the error criterion

$$E(\underline{q}, \underline{T}) = \int_{T_0}^{T_f} [d(t) - \underline{\alpha}^T(t; \underline{T}) \cdot \underline{q}]^2 dt \quad (4.24)$$

where

$$\underline{q}^T = (q_1, q_2, \dots, q_N) \quad (4.25)$$

$$\underline{\alpha}^T(t; \underline{T}) = (\alpha_1(t; \underline{T}), \alpha_2(t; \underline{T}), \dots, \alpha_N(t; \underline{T})) \quad (4.26)$$

and where the $(m+1)$ dimensional vector \underline{T} denote the set of parameters on which the simple functions $\alpha_i(t; \underline{T})$, $i = 1, 2, \dots, N$, depend. In the case of quadratic splines the vector \underline{T} represents the set of knots.

Since the argument \underline{q} occurs linearly inside the square brackets the error criterion $E(\underline{q}, \underline{T})$ can be minimized with respect to \underline{q} , holding \underline{T} fixed, to give an analytical expression for \underline{q} as a function of \underline{T} . Equation (4.24) can be rewritten as

$$\begin{aligned} E(\underline{q}, \underline{T}) &= \int_{T_0}^{T_f} [d^2(t) - d(t) \underline{\alpha}^T(t; \underline{T}) \cdot \underline{q}] dt \\ &\quad - \int_{T_0}^{T_f} [d(t) - \underline{\alpha}^T(t; \underline{T}) \cdot \underline{q}] \alpha^T(t; \underline{T}) \cdot \underline{q} dt \end{aligned} \quad (4.27)$$

Minimizing $E(\underline{q}, \underline{T})$ with respect to \underline{q} gives

$$\int_{T_0}^{T_f} [d(t) - \underline{\alpha}^T(t; \underline{T}) \cdot \underline{q}] \alpha_j^T(t; \underline{T}) dt = 0, \quad j = 1, 2, \dots, N \quad (4.28)$$

Or, equivalently, in matrix form

$$B(\underline{T}) \hat{\underline{q}}(\underline{T}) = \underline{\gamma}(\underline{T}) \quad (4.29)$$

where $\hat{\underline{q}}(\underline{T})$ denotes the optimum \underline{q} , the vector

$$\underline{\gamma}(\underline{T}) = (\gamma_1(\underline{T}), \gamma_2(\underline{T}), \dots, \gamma_N(\underline{T})) \quad (4.30)$$

has components

$$\gamma_j(\underline{T}) = \int_{T_0}^{T_f} d(t) \alpha_j(t; \underline{T}) dt, \quad j = 1, 2, \dots, N \quad (4.31)$$

and the matrix $B(\underline{T})$ has elements

$$b_{ij}(\underline{T}) = \int_{T_0}^{T_f} \alpha_i(t; \underline{T}) \alpha_j(t; \underline{T}) dt, \quad i, j = 1, 2, \dots, N \quad (4.32)$$

Substituting the optimum $\hat{\underline{q}}(\underline{T})$ into (4.27) gives

$$E(\hat{\underline{q}}(\underline{T}), \underline{T}) = \int_{T_0}^{T_f} d^2(t) dt - \int_{T_0}^T d(t) \underline{\alpha}^T(t, \underline{T}) \cdot \hat{\underline{q}}(\underline{T}) dt \quad (4.33)$$

since the second integral of (4.27) is zero by way of (4.28).

Using the definition of $\underline{\gamma}(\underline{T})$ we can rewrite (4.33) as

$$E(\hat{\underline{q}}(\underline{T}), \underline{T}) = \int_{T_0}^{T_f} d^2(t) dt - \underline{\gamma}^T(\underline{T}) \cdot \hat{\underline{q}}(\underline{T}) \quad (4.34)$$

Since the first term is independent of \underline{T} it will have no bearing on the generation of the optimum $\hat{\underline{T}}$. Consequently, we redefine the error criterion E as

$$E(\underline{T}) = \underline{\gamma}^T(\underline{T}) B^{-1}(\underline{T}) \underline{\gamma}(\underline{T}) \quad (4.35)$$

which is the last term of (4.34).

Our objective is to maximize (4.35) with respect to the knot vector \underline{T} in the presence of the constraints

$$T_{i-1} \leq T_i, \quad i = 1, 2, \dots, m+1 \quad (4.36)$$

where $T_{m+1} = T_f$.

4.4 VARIOUS CASES OF THE QUADRATIC SPLINE OPTIMIZATION PROBLEM

The quadratic spline function $r(t)$ is given by (4.14). In some problems the values of $r(T_o)$ and $r(T_f)$ are known a priori and in other problems the values of $r(T_o)$ and $\dot{r}(T_o)$ are known a priori. When this is the case such knowledge reduces the dimension of the coefficient vector \underline{q} . The following cases cover a spectrum of applications.

Case 1. No knowledge about $r(t)$ is known a priori. In this case

$$\underline{\alpha}(t; \underline{T}) = \underline{a}(t; \underline{T}) \quad (4.37)$$

$$\underline{q} = \underline{p} \quad (4.38)$$

Case 2. The values of $r(T_o)$ and $r(T_f)$ are known a priori:

$$r(T_o) = c_1 \quad (4.39)$$

$$r(T_f) = c_2 \quad (4.40)$$

For this case it is convenient to redefine the data $d(t)$ as

$$\tilde{d}(t) = d(t) - c_1 - (c_2 - c_1) \frac{(t - T_o)}{(T_f - T_o)} \quad (4.41)$$

and to define

$$\underline{q}^T = (\dot{r}_1, \dot{r}_2, \dots, \dot{r}_{m+1}) \quad (4.42)$$

and $\underline{\alpha}(t; \underline{T})$ with the components

$$\alpha_j(t; \underline{T}) = a_j(t; \underline{T}) - a_j(T_f; \underline{T}) \frac{(t - T_o)}{(T_f - T_o)} \quad (4.43)$$

for $j = 1, 2, \dots, m+1$. This case with $c_1 = c_2 = 0$ applies to the ship classification application.

Case 3. The values $r(T_o)$ and $\dot{r}(T_o)$ are known a priori:

$$r(T_o) = c_1 \quad (4.44)$$

$$\dot{r}(T_o) = c_3 \quad (4.45)$$

The data is redefined as

$$\tilde{d}(t) = d(t) - c_1 - c_3 (t - T_o) \quad (4.46)$$

In this case the vector function $\underline{\alpha}(t; \underline{T})$ and the coefficient vector \underline{q} are given by

$$\underline{\alpha}^T(t; \underline{T}) = (a_1(t; \underline{T}), a_2(t; \underline{T}), \dots, a_{m+1}(t; \underline{T})) \quad (4.47)$$

$$\underline{q}^T = (\ddot{r}_1, \ddot{r}_2, \dots, \ddot{r}_{m+1}) \quad (4.48)$$

Case 4. The value of $r(T_o)$ is given a priori:

$$r(T_o) = c_1 \quad (4.49)$$

The data $d(t)$ is redefined as

$$\tilde{d}(t) = d(t) - c_1 \quad (4.50)$$

The vector function $\underline{\alpha}(t, \underline{T})$ and the coefficient vector \underline{q} are defined as

$$\underline{\alpha}^T(t; \underline{T}) = (a_1(t; \underline{T}), a_2(t; \underline{T}), \dots, a_{m+1}(t; \underline{T}), a_{m+3}(t; \underline{T}) \quad (4.51)$$

$$\underline{q}^T = (\ddot{r}_1, \ddot{r}_2, \dots, \ddot{r}_{m+1}, \dot{r}_o) \quad (4.52)$$

Case 5. The value of $\dot{r}(T_o)$ and $r(T_f)$ are given a priori:

$$\dot{r}(T_o) = c_3 \quad (4.53)$$

$$r(T_f) = c_2 \quad (4.54)$$

The data $d(t)$ is redefined as

$$\tilde{d}(t) = d(t) - c_2 - c_3 (t - T_f) \quad (4.55)$$

The vector function $\underline{\alpha}(t, \underline{T})$ has components

$$\alpha_j(t; \underline{T}) = a_j(t; \underline{T}) - a_j(T_f; \underline{T}) \quad (4.56)$$

for $j = 1, 2, \dots, m+1$. The coefficient vector \underline{q} is defined as

$$\underline{q}^T = (\ddot{r}_1, \ddot{r}_2, \dots, \ddot{r}_{m+1}) \quad (4.57)$$

Case 6. The value of $\dot{r}(T_0)$ is given a priori

$$\dot{r}(T_0) = c_3$$

The data $d(t)$ is redefined as

$$\tilde{d}(t) = d(t) - c_3(t - T_0)$$

The vector function $\underline{a}(t, \underline{T})$ and the coefficient vector \underline{q} are defined as

$$\underline{a}^T(t; \underline{T}) = (a_1(t; \underline{T}), \dots, a_{m+2}(t; \underline{T}))$$

$$\underline{q}^T = (\ddot{r}_1, \ddot{r}_2, \dots, \ddot{r}_{m+1}, r_0)$$

CHAPTER V

SOLUTION TO POSED PROBLEM - AN OPTIMAL SPLINE METHOD

The problem is to maximize $E(\underline{T})$ of (4.35) with respect to the knot vector \underline{T} . Several gradient methods are available for carrying out the optimization: steepest descent, Newton-Raphson, Newton, Gauss-Newton, Fletcher-Powell and Davidon. Newton's method is appealing because of its quadratic convergence properties. It can be implemented since the Hessian matrix is analytically computable.

The derivative $\frac{\partial E(\underline{T})}{\partial \underline{T}}$ has a Taylor series expansion

$$\begin{aligned} \frac{\partial E(\underline{T}^b)}{\partial \underline{T}} &= \frac{\partial E(\underline{T}^a)}{\partial \underline{T}} + \frac{\partial^2 E(\underline{T}^a)}{\partial \underline{T}^2} (\underline{T}^b - \underline{T}^a) \\ &\quad + \text{higher order terms} \end{aligned} \quad (5.1)$$

If $E(\underline{T})$ has a maximum at $\underline{T} = \underline{T}^b$ then

$$\frac{\partial E(\underline{T}^b)}{\partial \underline{T}} = 0 \quad (5.2)$$

In addition, if the higher order terms are sufficiently small compared to the other terms of (5.1) then \underline{T}^b can be approximated by

$$\underline{T}^b = \underline{T}^a - \left[\frac{\partial^2 E(\underline{T}^a)}{\partial \underline{T}^2} \right]^{-1} \frac{\partial E(\underline{T}^a)}{\partial \underline{T}} \quad (5.3)$$

Sufficient conditions for the existence of a local maximum value of $E(\underline{T})$ at $\underline{T} = \underline{T}^b$ are given in [14, 15] and are that (5.2) is satisfied and that

$$D_i > 0, i = 2, 4, 6, \dots \quad (5.4)$$

$$D_i < 0, i = 1, 3, 5, \dots \quad (5.5)$$

where

$$D_i = \begin{vmatrix} E_{11} & E_{12} & \dots & E_{1i} \\ E_{21} & E_{22} & \dots & E_{2i} \\ \dots & \dots & \dots & \dots \\ E_{i1} & E_{i2} & \dots & E_{ii} \end{vmatrix} \quad (5.6)$$

$$E_{nk} = \frac{\partial^2 E(\underline{T}^b)}{\partial T_n \partial T_k}, n, k = 1, 2, \dots, i \quad (5.7)$$

Since the higher order terms are seldom zero the optimal value $\hat{\underline{T}}$ is obtained through convergence. That is, if $\underline{T}^a = \underline{T}^k$ represents the solution of (5.3) for the k^{th} iteration and if $\underline{T}^b = \underline{T}^{k+1}$ represents the solution of (5.3) for the $(k+1)^{\text{th}}$ iteration then

$$\hat{\underline{T}} = \lim_{k \rightarrow \infty} \underline{T}^{k+1} \quad (5.8)$$

Since

$$\hat{\underline{q}}(\underline{T}) = B^{-1}(\underline{T}) \underline{\gamma}(\underline{T}) \quad (5.9)$$

we can rewrite $E(\underline{T})$ in the following forms

$$E(\underline{T}) = \underline{\hat{q}}^T(\underline{T}) \underline{\gamma}(\underline{T}) \quad (5.10)$$

$$= \underline{\gamma}^T(\underline{T}) \underline{\hat{q}}(\underline{T}) \quad (5.11)$$

In much of the following development the argument \underline{T} will be left out of the various functions such as E , $\underline{\hat{q}}$, $\underline{\gamma}$, B and their derivatives.

The vector $\frac{\partial E}{\partial \underline{T}}$ has components $\frac{\partial E}{\partial T_1}, \frac{\partial E}{\partial T_2}, \dots, \frac{\partial E}{\partial T_m}$

These components are given by, $k = 1, 2, \dots, m$,

$$\frac{\partial E}{\partial T_k} = 2 \underline{\hat{q}}^T \frac{\partial \underline{\gamma}}{\partial T_k} - \underline{\hat{q}}^T \frac{\partial B}{\partial T_k} \underline{\hat{q}} \quad (5.12)$$

which is obtained by use of the identity

$$\frac{\partial B^{-1}}{\partial T_k} = -B^{-1} \frac{\partial B}{\partial T_k} B^{-1} \quad (5.13)$$

The elements of the matrix $\frac{\partial^2 E}{\partial \underline{T}^2}$ are

given by, $k, n = 1, 2, \dots, m$,

$$\begin{aligned} \frac{\partial^2 E}{\partial T_k \partial T_n} = & 2 \left\{ \frac{\partial \underline{\gamma}^T}{\partial T_n} B^{-1} \frac{\partial \underline{\gamma}}{\partial T_k} + \underline{\hat{q}}^T \frac{\partial^2 \underline{\gamma}}{\partial T_k \partial T_n} \right. \\ & - \underline{\hat{q}}^T \frac{\partial B}{\partial T_n} B^{-1} \frac{\partial \underline{\gamma}}{\partial T_k} - \underline{\hat{q}}^T \frac{\partial B}{\partial T_k} B^{-1} \frac{\partial \underline{\gamma}}{\partial T_n} \\ & \left. + \underline{\hat{q}}^T \frac{\partial B}{\partial T_k} B^{-1} \frac{\partial B}{\partial T_n} \underline{\hat{q}} - \frac{1}{2} \underline{\hat{q}}^T \frac{\partial^2 B}{\partial T_k \partial T_n} \underline{\hat{q}} \right\} \quad (5.14) \end{aligned}$$

Consequently, in order to solve (5.3) we need the following computed for $k, n = 1, 2, \dots, m$:

$$\gamma, B, B^{-1}, \hat{q}$$

$$\frac{\partial \gamma}{\partial T_k}, \frac{\partial B}{\partial T_k}$$

$$\frac{\partial^2 \gamma}{\partial T_k \partial T_n}, \frac{\partial^2 B}{\partial T_k \partial T_n}$$

Expressions for the above quantities can be derived for each case discussed in Section 4.4. These expressions are derived for Case 1 in Chapters VI and VII.

CHAPTER VI

ANALYTICAL EXPRESSIONS FOR THE QUANTITIES OF CASE 1

6.1 The B Matrix

The elements of the symmetric matrix B are given by

$$b_{ji} = \int_{T_o}^{T_f} a_j(t) a_i(t) dt$$

for $j, i = 1, 2, \dots, m+3$ where the a 's are defined by (4.18) - (4.20).

The argument T has been dropped.

For $i = 1, 2, \dots, m+1$, define

$$Z_i = T_i - T_{i-1} \quad (6.1)$$

$$S_i = T_f - T_i \quad (6.2)$$

For $i = 1, 2, \dots, m+1$ the following equations can be derived:

$$b_{ii} = \frac{Z_i^5}{20} + \frac{Z_i^4}{4} S_i + \frac{Z_i^3}{2} S_i^2 + \frac{Z_i^2}{3} S_i^3 \quad (6.3)$$

For $i = 1, 2, \dots, m$ the following equation holds:

$$b_{i(i+1)} = Z_i Z_{i+1} \left\{ \frac{Z_{i+1}^2}{12} \left[\frac{Z_{i+1}}{2} + Z_f \right] + \frac{S_i^3}{3} + \frac{S_i}{4} [Z_i S_{i+1} - Z_{i+1} S_i] \right\} \quad (6.4)$$

The following equation has been derived for $i = 1, 2, \dots, m-1$;

$j = i + 2, \dots, m + 1$:

$$b_{ij} = \frac{Z_i Z_j}{2} \left\{ (S_i + \frac{Z_i}{2}) [S_j (S_j + Z_j) + \frac{Z_j^2}{3}] + \right. \\ \left. - \frac{(S_{j-1}^2 + Z_j^2)}{3} (S_j - \frac{Z_j}{2}) - \frac{5}{12} Z_j^3 \right\} \quad (6.5)$$

Equations (6.6) and 6.7) hold for $i = 1, 2, \dots, m+1$.

$$b_{i(m+2)} = \frac{Z_i^3}{6} + \frac{Z_i^2}{2} S_i + \frac{Z_i}{2} S_i^2 \quad (6.6)$$

$$b_{i(m+3)} = [T_f - T_o - S_i] b_{i(m+2)} + \\ - \frac{Z_i^4}{24} + \frac{Z_i^2}{4} S_i^2 + \frac{Z_i S_i^3}{3} \quad (6.7)$$

$$b_{(m+2)(m+2)} = T_f - T_o \quad (6.8)$$

$$b_{(m+2)(m+3)} = \frac{(T_f - T_o)^2}{2} \quad (6.9)$$

$$b_{(m+3)(m+3)} = \frac{(T_f - T_o)^3}{3} \quad (6.10)$$

6.2 The $\frac{\partial B}{\partial T_k}$ Matrix

The elements of $\frac{\partial B}{\partial T_k}$ are denoted by

$$\frac{\partial b_{ij}}{\partial T_k} = b_{ij, k} \quad (6.11)$$

Note that

$$b_{ij, k} = 0 \text{ unless } i, j = k \text{ or } k+1 \quad (6.12)$$

The following equations, (6.13) - (6.23), hold for
 $k = 1, 2, \dots, m$:

In addition, Equations (6.13) and (6.14) hold for $j = 1, 2, \dots, k-1$:

$$b_{jk, k} = \frac{Z_j}{2} S_k^2 \left(S_j - \frac{S_k}{3} + \frac{Z_j}{2} \right) \quad (6.13)$$

$$b_{j(k+1), k} = -b_{jk, k} \quad (6.14)$$

$$b_{kk, k} = Z_k S_k^2 \left(\frac{2 S_k}{3} + \frac{Z_k}{2} \right) \quad (6.15)$$

$$b_{k(k+1), k} = \frac{Z_{k+1}^4}{24} + \frac{S_k^2}{4} \left(\frac{4 S_k}{3} (Z_{k+1} - Z_k) \right. \quad (6.16)$$

$$\left. - Z_{k+1}^2 - Z_k^2 \right)$$

$$b_{(k+1)(k+1), k} = -\frac{Z_{k+1}^4}{12} - S_k^2 Z_{k+1} \quad (6.17)$$

$$\left(\frac{2}{3} S_k - \frac{Z_{k+1}}{2} \right)$$

Note that

$$b_{kk, k} + b_{(k+1)(k+1), k} = -2 b_{k(k+1), k}$$

Equations (6.18) and (6.19) hold for $j = k+2, \dots, m+1$:

$$b_{kj, k} = \frac{Z_j}{2} \left\{ S_k [S_j S_{j-1} + \frac{Z_j^2}{3}] - \left(\frac{S_{j-1}^2 + Z_j^2}{3} \right) \left(S_j - \frac{Z_j}{2} \right) - \frac{5}{12} Z_j^3 \right\} \quad (6.18)$$

$$b_{(k+1)j, k} = -b_{kj, k} \quad (6.19)$$

$$b_{k(m+2), k} = \frac{S_k^2}{2} \quad (6.20)$$

$$b_{k(m+3), k} = -\frac{S_k^3}{6} + \frac{S_k^2}{2} (T_f - T_o) \quad (6.21)$$

$$b_{(k+1)(m+2), k} = -b_{k(m+2), k} \quad (6.22)$$

$$b_{(k+1)(m+3), k} = -b_{k(m+3), k} \quad (6.23)$$

6.3 The $\frac{\partial^2 B}{\partial T_k \partial T_n}$ Matrix for $k = n$; $n = 1, 2, \dots, m$.

The elements of $\frac{\partial^2 B}{\partial T_n^2}$ are denoted by

$$\frac{\partial^2 b_{ij}}{\partial T_n^2} = b_{ij, nn}$$

Note that

$$\frac{\partial^2 b_{ij}}{\partial T_n^2} = 0 \text{ unless } i \text{ or } j = n \text{ or } n+1 \quad (6.24)$$

Equations (6.25) and (6.26) hold for $i = 1, 2, \dots, n-1$:

$$b_{in, nn} = - \frac{Z_i S_n}{2} (S_i + S_{i-1} - S_n) \quad (6.25)$$

$$b_{i(n+1), nn} = - b_{in, nn} \quad (6.26)$$

$$b_{nn, nn} = - Z_n S_n S_{n-1} + \frac{2S_n^3}{3} \quad (6.27)$$

$$b_{(n+1)(n+1), nn} = Z_{n+1} S_n S_{n+1} + \frac{Z_{n+1}^3}{3} + \frac{2S_n^3}{3} \quad (6.28)$$

$$b_{n(n+1), nn} = - \frac{b_{nn, nn} + b_{(n+1)(n+1), nn}}{2} \quad (6.29)$$

Equations (6.30) and (6.31) hold for $j = n+2, \dots, m+1$:

$$b_{nj, nn} = - \frac{Z_j^3}{6} - \frac{Z_j}{2} S_j S_{j-1} \quad (6.30)$$

$$b_{(n+1)j, nn} = - b_{nj, nn} \quad (6.31)$$

$$b_{n(m+2), nn} = - S_n \quad (6.32)$$

$$b_{n(m+3), nn} = \frac{S_n^2}{2} - S_n (T_f - T_o) \quad (6.33)$$

$$b_{(n+1)(m+2), nn} = - b_{n(m+2), nn} \quad (6.34)$$

$$b_{(n+1)(m+3), nn} = - b_{n(m+3), nn} \quad (6.35)$$

6.4 The $\frac{\partial^2 B}{\partial T_k \partial T_n}$ Matrix for $k = n+1; n = 1, 2, \dots, m-1$.

The elements of $\frac{\partial^2 B}{\partial T_{n+1} \partial T_n}$ are denoted by $b_{ij, (n+1) n}$.

Note that

$$b_{ij, (n+1) n} = 0 \text{ unless } i \text{ and } j = n, n+1 \text{ or } n+2 \quad (6.36)$$

$$b_{nn, (n+1) n} = 0 \quad (6.37)$$

$$b_{n(n+1), (n+1) n} = S_{n+1}^2 \left(\frac{S_{n+1}}{3} + \frac{Z_{n+1}}{2} \right) \quad (6.38)$$

$$b_{n(n+2), (n+1) n} = -b_{n(n+1), (n+1) n} \quad (6.39)$$

$$b_{(n+1)n, (n+1) n} = b_{n(n+1), (n+1) n} \quad (6.40)$$

$$b_{(n+1)(n+1), (n+1) n} = -2b_{n(n+1), (n+1) n} \quad (6.41)$$

$$b_{(n+1)(n+2), (n+1) n} = b_{n(n+1), (n+1) n} \quad (6.42)$$

$$b_{(n+2)n, (n+1) n} = -b_{n(n+1), (n+1) n} \quad (6.43)$$

$$b_{(n+2)(n+1), (n+1) n} = b_{n(n+1), (n+1) n} \quad (6.44)$$

$$b_{(n+2)(n+2), (n+1) n} = 0 \quad (6.45)$$

6.5 The $\frac{\partial^2 B}{\partial T_k \partial T_n}$ Matrix for $k = n+2, \dots, m; n = 1, 2, \dots, m-2$

The elements of $\frac{\partial^2 B}{\partial T_k \partial T_n}$ are denoted by $b_{ij, kn}$.

Since B is symmetric we consider only those elements b_{ij} with $i \leq j$.

$$b_{ij, kn} = 0 \text{ unless } i = n \text{ or } n+1 \text{ and } j = k \text{ or } k+1 \quad (6.46)$$

$$b_{nk, kn} = S_k^2 \left(\frac{S_n}{2} - \frac{S_k}{6} \right) \quad (6.47)$$

$$b_{n(k+1), kn} = -b_{nk, kn} \quad (6.48)$$

$$b_{(n+1)k, kn} = -b_{nk, kn} \quad (6.49)$$

$$b_{(n+1)(k+1), kn} = b_{nk, kn} \quad (6.50)$$

6.6 The $\underline{\gamma}$ Vector

The elements of $\underline{\gamma}$ are given by

$$\gamma_j = \int_{T_0}^{T_f} d(t) a_j(t) dt \quad (6.51)$$

for $j = 1, 2, \dots, m+3$. Since the data $d(t)$ is given in discrete form rather than continuously we write the discrete form of (6.51) as

$$\gamma_j = \frac{T_f - T_0}{I} \sum_{i=1}^I d_i a_j(t_i) \quad (6.52)$$

where I is the number of data points and where

$$d_i = d(t_i), i = 1, 2, \dots, I \quad (6.53)$$

$$t_{i+1} = t_i + \Delta t \quad (6.54)$$

$$\Delta t = \frac{T_f - T_o}{I} \quad (6.55)$$

$$t_1 = T_o + \frac{\Delta t}{2} \quad (6.56)$$

$$t_I = T_f - \frac{\Delta t}{2} \quad (6.57)$$

For $j = 1, 2, \dots, m$ define the integer $J(j)$ so that it satisfies the inequalities

$$t_{J(j)} \leq T_j < t_{J(j)+1} \quad (6.58)$$

Consequently, γ_1 is given by

$$\gamma_1 = \frac{(T_f - T_o)}{I} \left\{ \sum_{i=1}^{J(1)} d_i \frac{(t_i - T_o)^2}{2} + \sum_{i=J(1)+1}^I d_i \right\} \quad (6.59)$$

$$Z_1 \sum_{i=J(1)+1}^I d_i t_i + Z_1 \left(\frac{Z_1}{2} - T_1 \right)$$

For $j = 2, 3, \dots, m$, γ_j is given by

$$\gamma_j = \frac{(T_f - T_o)}{I} \left\{ \sum_{i=J(j-1)+1}^{J(j)} d_i \frac{(t_i - T_{j-1})^2}{2} + \sum_{i=J(j)+1}^I d_i \right\} \quad (6.60)$$

$$Z_j \sum_{i=J(j)+1}^I d_i t_i + Z_j \left(\frac{Z_j}{2} - T_j \right)$$

Furthermore, γ_{m+1} is given by

$$\gamma_{m+1} = \frac{(T_f - T_o)}{I} \sum_{i=J(m)+1}^I d_i \frac{(t_i - T_m)^2}{2} \quad (6.61)$$

and, γ_{m+2} and γ_{m+3} have the equations

$$\gamma_{m+2} = \frac{(T_f - T_o)}{I} \sum_{i=1}^I d_i \quad (6.62)$$

$$\gamma_{m+3} = \frac{(T_f - T_o)}{I} \sum_{i=1}^I d_i (t_i - T_o) \quad (6.63)$$

6.7 The $\frac{\partial \gamma}{\partial T_k}$ Vector for $k = 1, 2, \dots, m$

The elements of $\frac{\partial \gamma}{\partial T_k}$ are denoted by

$$\frac{\partial \gamma_j}{\partial T_k} = \gamma_{j, k} \quad (6.64)$$

From (6.59) - (6.61) we derive

$$\gamma_{j, k} = 0 \quad j = 1, 2, \dots, k-1 \quad (6.65)$$

$$\gamma_{k, k} = \frac{(T_f - T_o)}{I} \sum_{i=J(k)+1}^I d_i (t_i - T_k) \quad (6.66)$$

$$\gamma_{(k+1), k} = - \gamma_{k, k} \quad (6.67)$$

$$\gamma_{j, k} = 0 \quad j = k+2, \dots, m+3 \quad (6.68)$$

6.8 The $\frac{\partial^2 \gamma}{\partial T_k \partial T_n}$ Vector for $n=1, 2, \dots, m$; $k=n, n+1, \dots, m$

The elements of $\frac{\partial^2 \gamma}{\partial T_k \partial T_n}$ are denoted by

$$\frac{\partial^2 \gamma_j}{\partial T_k \partial T_n} = \gamma_{j, kn} \quad (6.69)$$

For $k \neq n$ we note that

$$\gamma_{j, kn} = 0, \quad j = 1, 2, \dots, m+3 \quad (6.70)$$

For $k = n$ we can check that

$$\gamma_{j, nn} = 0 \text{ unless } j = n \text{ or } n+1 \quad (6.71)$$

$$\gamma_{n, nn} = - \frac{(T_f - T_o)}{I} \sum_{i=J(n)+1}^I d_i \quad (6.72)$$

$$\gamma_{(n+1), nn} = - \gamma_{n, nn} \quad (6.73)$$

CHAPTER VII

ANALYTICAL EXPRESSIONS FOR $\frac{\partial E}{\partial T_k}$ AND $\frac{\partial^2 E}{\partial T_k \partial T_n}$

In Section 6.7 it is shown that the vector $\frac{\partial \gamma}{\partial T_k}$ has at most two nonzero components. In Section 6.2 it is shown that the matrix $\frac{\partial B}{\partial T_k}$ has at most two nonzero rows and two nonzero columns. The sparseness of the nonzero elements in these vectors and matrices greatly facilitates the calculations of $\frac{\partial E}{\partial T_k}$ and $\frac{\partial^2 E}{\partial T_k \partial T_n}$. The formulas for these derivatives are given in this section.

It is convenient to make the following definitions for $n = 1, 2, \dots, m$;
 $k = 1, 2, \dots, m$:

$$A_n = \sum_{j=1}^{m+3} b_{jn, n} q_j - (q_n - q_{n+1}) b_{nn, n} \quad (7.1)$$

$$C_n = \sum_{i=1}^{m+3} b_{in, nn} q_i - \frac{(q_n - q_{n+1}) b_{nn, nn}}{2} \quad (7.2)$$

$$f_{nk} = h_{nk} - h_{n(k+1)} + h_{(n+1)(k+1)} \quad (7.3)$$

$$F_{nk} = \sum_{i=1}^{m+3} \sum_{j=1}^{m+3} b_{in, n} b_{jk, k} h_{ij} \quad (7.4)$$

$$G_{nk} = \sum_{i=1}^{m+3} b_{in, n} (h_{ik} - h_{i(k+1)}) \quad (7.5)$$

where the matrix H is given by

$$H = B^{-1} \quad (7.6)$$

with elements h_{ij} , $i, j = 1, 2, \dots, m+3$.

Note that

$$b_{kk, k} + b_{(k+1)(k+1), k} = -2 b_{k(k+1), k} \quad (7.7)$$

$$b_{nn, nn} + b_{(n+1)(n+1), nn} = -2 b_{n(n+1), nn} \quad (7.8)$$

The following analytical expressions have been derived, having made use of (7.7) and (7.8):

$$\frac{\partial \gamma}{\partial T_k} = (q_k - q_{k+1}) \gamma_{k, k} \quad (7.9)$$

$$\frac{\partial B}{\partial T_k} = 2(q_k - q_{k+1}) A_k + (q_k - q_{k+1})^2 b_{kk, k} \quad (7.10)$$

$$\frac{\partial E}{\partial T_k} = 2(q_k - q_{k+1}) (\gamma_{k, k} - A_k) - (q_k - q_{k+1})^2 b_{kk, k} \quad (7.11)$$

$$\frac{\partial^2 \gamma}{\partial T_k \partial T_n} = 0 \text{ for } k \neq n \quad (7.12)$$

$$\frac{\partial^2 \gamma}{\partial T_n^2} = \gamma_{n, nn} (q_n - q_{n+1}) \quad (7.13)$$

$$\frac{\partial \gamma}{\partial T_n} B^{-1} \frac{\partial \gamma}{\partial T_k} = \gamma_{n, n} \gamma_{k, k} f_{nk} \quad (7.14)$$

$$\frac{\partial B}{\partial T_k} B^{-1} \frac{\partial \gamma}{\partial T_k} = \gamma_{k, k} [(q_n - q_{n+1}) G_{nk} + f_{nk} A_n] \quad (7.15)$$

$$\frac{\partial B}{\partial T_k} B^{-1} \frac{\partial \gamma}{\partial T_n} = \gamma_{n, n} [(q_k - q_{k+1}) G_{kn} + f_{nk} A_k] \quad (7.16)$$

For $n = 1, 2, \dots, m-1$ and $k = n+1, n+2, \dots, m$ it can be shown that (7.17) holds:

$$\frac{\partial^2 B}{\partial T_k \partial T_n} = 2 b_{nk, kn} (q_n - q_{n+1}) (q_k - q_{k+1}) \quad (7.17)$$

For $n = k$ it can be verified that (7.18) holds:

$$\frac{\partial^2 B}{\partial T_n^2} = 2(q_n - q_{n+1}) C_n \quad (7.18)$$

$$\begin{aligned} \frac{\partial B}{\partial T_n} B^{-1} \frac{\partial B}{\partial T_k} &= A_n A_k f_{nk} + (q_n - q_{n+1}) A_k G_{nk} + \\ &+ (q_k - q_{k+1}) A_n G_{kn} + (q_n - q_{n+1}) (q_k - q_{k+1}) F_{nk} \end{aligned} \quad (7.19)$$

Consequently, it follows from (7.12), (7.14) - (7.17) and (7.19) that the following Equation (7.20) holds for $k = n$ and Equation (7.21) holds for $k \neq n$:

$$\begin{aligned} \frac{\partial^2 E}{\partial T_n^2} &= 2 \{ f_{nn} (A_n - \gamma_{n, n})^2 + \\ &+ (q_n - q_{n+1}) [\gamma_{n, nn} - C_n + (q_n - q_{n+1}) F_{nn} + \\ &+ 2 G_{nn} (A_n - \gamma_{n, n})] \} \end{aligned} \quad (7.20)$$

$$\begin{aligned}
\frac{\partial^2 E}{\partial T_k \partial T_n} &= 2 \{ f_{nk} (A_n - \gamma_{n, n}) (A_k - \gamma_{k, k}) + \\
&(q_n - q_{n+1}) (q_k - q_{k+1}) (F_{nk} - b_{nk, kn}) + \\
&(q_k - q_{k+1}) G_{kn} (A_n - \gamma_{n, n}) + \\
&(q_n - q_{n+1}) G_{nk} (A_k - \gamma_{k, k}) \} \quad (7.21)
\end{aligned}$$

CHAPTER VIII

ANALYTICAL EXPRESSIONS FOR THE QUANTITIES OF THE SHIP CLASSIFICATION CASE - CASE 2.

8.1 The B Matrix

The elements of the symmetric matrix B are given by

$$\beta_{ij} = \int_{T_o}^{T_f} \alpha_i(t) \alpha_j(t) dt \quad i, j = 1, 2, \dots, m+1 \quad (8.1)$$

where the α 's are defined by (4.43). Integrating (8.1) after the substitution of (4.43) gives

$$\begin{aligned} \beta_{ij} = & b_{ij} + \frac{a_i a_j b_{(m+3)}(m+3)}{(T_f - T_o)^2} - \frac{a_i b_j(m+3)}{(T_f - T_o)} \\ & - \frac{a_j b_i(m+3)}{(T_f - T_o)}, \quad i, j = 1, 2, \dots, m+1 \end{aligned} \quad (8.2)$$

where b_{ij} is defined in Section 6.1 and where

$$a_i = Z_i \left(S_i + \frac{Z_i}{2} \right), \quad i = 1, 2, \dots, m+1 \quad (8.3)$$

8.2 The $\frac{\partial B}{\partial T_k}$ Matrix

The elements of $\frac{\partial B}{\partial T_k}$ are denoted by

$$\frac{\partial \beta_{ij}}{\partial T_k} = \beta_{ij, k} \quad (8.4)$$

Note that

$$\beta_{ij, k} = 0 \text{ unless } i, j = k \text{ or } k+1 \quad (8.5)$$

The following equations, (8.6) - (8.10), hold for $k = 1, 2, \dots, m$:

Equations (8.6) and (8.7) hold for $j = 1, 2, \dots, k-1$ and for $j = k+2, \dots, m+1$.

$$\begin{aligned} \beta_{jk, k} &= b_{jk, k} + \frac{a_j S_k}{(T_f - T_o)^2} b_{(m+3)(m+3)} + \\ &- \frac{S_k b_{j(m+3)}}{(T_f - T_o)} - \frac{a_j}{(T_f - T_o)} b_{(m+3)k, k} \end{aligned} \quad (8.6)$$

$$\beta_{j(k+1), k} = -\beta_{jk, k} \quad (8.7)$$

$$\begin{aligned} \beta_{kk, k} &= b_{kk, k} + \frac{2a_k S_k}{(T_f - T_o)^2} b_{(m+3)(m+3)} - \frac{2S_k b_{k(m+3)}}{(T_f - T_o)} + \\ &- \frac{2b_{(m+3)k, k} a_k}{(T_f - T_o)} \end{aligned} \quad (8.8)$$

$$\begin{aligned} \beta_{(k+1)k, k} &= b_{(k+1)k, k} + \frac{b_{(m+3)(m+3)}}{(T_f - T_o)^2} (a_{k+1} - a_k) S_k + \\ &- \frac{b_{(m+3)k, k}}{(T_f - T_o)} (a_{k+1} - a_k) + \\ &\frac{S_k}{(T_f - T_o)} (b_{(m+3)k} - b_{(m+3)(k+1)}) \end{aligned} \quad (8.9)$$

$$\beta_{kk, k} + \beta_{(k+1)(k+1), k} = -2\beta_{(k+1)k, k} \quad (8.10)$$

8.3 The $\frac{\partial^2 B}{\partial T_k \partial T_n}$ Matrix for $k = n; n = 1, 2, \dots, m$

The elements of $\frac{\partial^2 B}{\partial T_n^2}$ are denoted by

$$\frac{\partial^2 \beta_{ij}}{\partial T_n^2} = \beta_{ij, nn}$$

Note that

$$\frac{\partial^2 \beta_{ij}}{\partial T_n^2} = 0 \quad \text{unless } i \text{ or } j = n \text{ or } n+1 \quad (8.11)$$

Equations (8.12) and (8.13) hold for $i = 1, 2, \dots, n-1, n-2, \dots, m+1$:

$$\begin{aligned} \beta_{in, nn} &= b_{in, nn} - \left(a_i \frac{b_{(m+3)(m+3)}}{(T_f - T_o)^2} - \frac{b_{i(m+3)}}{(T_f - T_o)} \right) \\ &\quad - a_i \frac{b_{(m+3)n, nn}}{(T_f - T_o)} \end{aligned} \quad (8.12)$$

$$\beta_{i(n+1), nn} = -\beta_{in, nn} \quad (8.13)$$

$$\begin{aligned} \beta_{nn, nn} &= b_{nn, nn} + 2 \left\{ \frac{S_n^2 b_{(m+3)(m+3)}}{(T_f - T_o)^2} - \frac{a_n b_{(m+3)(m+3)}}{(T_f - T_o)^2} + \right. \\ &\quad \left. \frac{b_{(m+3)n}}{(T_f - T_o)} - \frac{2S_n b_{(m+3)n, n}}{(T_f - T_o)} - \frac{a_n b_{(m+3)n, nn}}{(T_f - T_o)} \right\} \end{aligned} \quad (8.14)$$

$$\beta_{(n+1)n, nn} = b_{(n+1)n, nn} + \frac{b_{(m+3)(m+3)}}{(T_f - T_o)^2} \{ a_n - a_{n+1} - 2S_n^2 \} +$$

$$\frac{1}{(T_f - T_o)} \{ b_{(m+3)(n+1)} - b_{(m+3)n} + b_{(m+3)n, nn} (a_n - a_{n+1}) + 4S_n b_{(m+3)n, n} \} \quad (8.15)$$

$$\beta_{nn, nn} + \beta_{(n+1)(n+1), nn} = -2\beta_{(n+1)n, nn} \quad (8.16)$$

8.4 The $\frac{\partial^2 B}{\partial T_k \partial T_n}$ Matrix for $k = n+1; n = 1, 2, \dots, m-1$.

The elements of $\frac{\partial^2 B}{\partial T_{n+1} \partial T_n}$ are denoted by

$$\frac{\partial^2 \beta_{ij}}{\partial T_{n+1} \partial T_n} = \beta_{ij, (n+1)n} \quad (8.17)$$

Note that

$$\beta_{ij, (n+1)n} = 0 \quad \text{unless } i \text{ and } j = n, n+1 \text{ or } n+2 \quad (8.18)$$

$$\beta_{nn, (n+1)} = 0$$

$$\begin{aligned} \beta_{(n+1)n, (n+1)n} &= b_{(n+1)n, (n+1)n} + \frac{S_n S_{n+1}}{(T_f - T_o)^2} b_{(m+3)(m+3)} + \\ &- \frac{1}{(T_f - T_o)} [S_{n+1} b_{(m+3)n, n} + S_n b_{(m+3)(n+1), n+1}] \quad (8.19) \end{aligned}$$

$$\beta_{n(n+2), (n+1)n} = -\beta_{n(n+1), (n+1)n} \quad (8.20)$$

$$\beta_{(n+1)n, (n+1)n} = \beta_{n(n+1), (n+1)n} \quad (8.21)$$

$$\beta_{(n+1)(n+1), (n+1)n} = -2\beta_{n(n+1), (n+1)n} \quad (8.22)$$

$$\beta_{(n+1)(n+2), (n+1)n} = \beta_{n(n+1), (n+1)n} \quad (8.23)$$

$$\beta_{(n+2)n, (n+1)n} = -\beta_{n(n+1), (n+1)n} \quad (8.24)$$

$$\beta_{(n+2)(n+1), (n+1)n} = \beta_{n(n+1), (n+1)n} \quad (8.25)$$

$$\beta_{(n+2)(n+2), (n+1)n} = 0 \quad (8.26)$$

8.5 The $\frac{\partial^2 B}{\partial T_k \partial T_n}$ Matrix for $k = n+2, \dots, m; n = 1, 2, \dots, m-2$.

The elements of $\frac{\partial^2 B}{\partial T_k \partial T_n}$ are denoted by

$$\frac{\partial^2 \beta_{ij, kn}}{\partial T_k \partial T_n} = \beta_{ij, kn} \quad (8.27)$$

Since B is symmetric we consider only those elements β_{ij} with $i \leq j$.

$$\beta_{ij, kn} = 0 \quad \text{unless } i = n \text{ or } n+1 \text{ and } j = k \text{ or } k+1 \quad (8.28)$$

$$\beta_{nk, nk} = b_{nk, nk} - \frac{S_k b_{(m+3)n, n}}{(T_f - T_o)} +$$

$$S_n \left[\frac{S_k b_{(m+3)(m+3)}}{(T_f - T_o)^2} - \frac{b_{(m+3)k, k}}{(T_f - T_o)} \right] \quad (8.29)$$

8.6 The $\underline{\delta}$ Vector

The elements of $\underline{\delta}$ are given by

$$\delta_j = \int_{T_o}^{T_f} d(t) \alpha_j(t) dt \quad (8.30)$$

for $j = 1, 2, \dots, m+1$. Making use of (4.43) we obtain

$$\delta_j = \gamma_j - \frac{a_j \gamma_{m+3}}{(T_f - T_o)}, \quad j = 1, 2, \dots, m+1 \quad (8.31)$$

8.7 The $\frac{\partial \underline{\delta}}{\partial T_k}$ Vector for $k = 1, 2, \dots, m$.

The elements of $\frac{\partial \underline{\delta}}{\partial T_k}$ are denoted by

$$\frac{\partial \delta_j}{\partial T_k} = \delta_{j, k} \quad (8.32)$$

It can be shown that

$$\delta_{j, k} = 0 \quad j = 1, 2, \dots, k-1, k+2, \dots, m+1 \quad (8.33)$$

The Equations (8.34) and (8.35) hold for $j = 1, 2, \dots, m$:

$$\delta_{j, j} = \gamma_{j, j} - \frac{S_j}{(T_f - T_o)} \alpha_{m+3} \quad (8.34)$$

$$\delta_{(j+1), j} = -\delta_{j, j} \quad (8.35)$$

8.8 The $\frac{\partial^2 \delta}{\partial T_k \partial T_n}$ Vector for $n = 1, 2, \dots, m; k = n, n+1, \dots, m$.

The elements of $\frac{\partial^2 \delta}{\partial T_k \partial T_n}$ are denoted by

$$\frac{\partial^2 \delta_j}{\partial T_k \partial T_n} = \delta_{j, kn} \quad (8.36)$$

For $k \neq n$ we note that

$$\delta_{j, kn} = 0, \quad j = 1, 2, \dots, m+1 \quad (8.37)$$

For $k = n$ we can verify that

$$\delta_{j, nn} = 0 \quad \text{unless } j = n \text{ or } n+1 \quad (8.38)$$

$$\delta_{n, nn} = \gamma_{n, nn} + \frac{\gamma_{m+3}}{(T_f - T_o)} \quad (8.39)$$

$$\delta_{(n+1), nn} = -\delta_{n, nn} \quad (8.40)$$

The analytical expression of $\frac{\partial E}{\partial T_k}$ and $\frac{\partial^2 E}{\partial T_k \partial T_n}$ for Case 2 have the same form as given in Chapter VII. It is only necessary to substitute $\underline{\delta}$ for $\underline{\gamma}$ and β for b . It is important to modify the data $d(t)$ according to Equation (4.41) before computing the vector $\underline{\delta}$ and its derivatives of Section 6.6 - 6.8 for their use in Sections 8.6 - 8.8.

CHAPTER IX

ANALYTICAL EXPRESSIONS FOR THE QUANTITIES OF CASES 3-6.

The analytical expressions for Cases 3 and 4 are the same as for Case 1; the only differences are (1) the dimension of the vectors \underline{q} and \underline{a} and (2) the summations of Equations (7.1, 7.2, 7.4 and 7.5) are carried out over the dimension of \underline{q} . Case 6 is similar.

9.1 The B Matrix for Case 5

The elements of the symmetric matrix B are given by

$$\beta_{ij} = b_{ij} - a_j b_{(m+2)i} - a_i b_{(m+2)j} + a_i a_j b_{(m+2)(m+2)} \quad (9.1)$$

where the a_i 's are defined by (8.3) and the b's are given in Section 6.1. Comparing (9.1) with (8.2) we note that the analytical expressions of B and its derivatives have the same form as in Case 2; it is only necessary to make the following substitutions together with their partial derivatives:

$$\text{substitute } b_{(m+2)(m+2)} \text{ for } \frac{b_{(m+3)(m+3)}}{(T_f - T_o)^2} \quad (9.2)$$

$$\text{substitute } b_{j(m+2)} \text{ for } \frac{b_{j(m+3)}}{(T_f - T_o)} \quad (9.3)$$

9.2 The $\underline{\delta}$ Vector for Case 5

The elements of $\underline{\delta}$ are given by

$$\delta_j = \gamma_j - a_j \gamma_{m+2}, \quad j = 1, 2, \dots, m+1 \quad (9.4)$$

Consequently, in view of Equation (8.31) the analytical expressions for $\underline{\delta}$ and its derivatives in Case 5 have the same form as Case 2; it is only necessary to make the following substitution together with its derivatives:

$$\text{substitute } \gamma_{m+2} \text{ for } \frac{\gamma_{m+3}}{(T_f - T_o)} \quad (9.5)$$

It is necessary to modify the data $d(t)$ according to Equations (4.46, 4.50 and 4.55) before computing the $\underline{\gamma}$ and its derivatives of Sections 6.6 - 6.8 for their use in Cases 3-5.

CHAPTER X

PROCEDURE FOR STARTING ESTIMATES OF KNOTS

In this section we describe a method for generating a starting estimate for the minimum number of knots and starting estimates for the knot values.

10.1 A Procedure for Estimating the Minimum Number of Knots

Let M be an integer and let the knots \widetilde{T}_i , $i = 1, 2, \dots, M$ be equally spaced across the time interval $[T_0, T_f]$. Equation (4.29) or (5.9) can be solved for the values of q_i , $i = 1, 2, \dots, M+3$. The error $E(\underline{q}, \widetilde{T})$ can be computed using Equation (4.24). If the error falls outside a required degree of accuracy then the value of M is increased until the computed error lies within a required degree of accuracy. When this is the case the spline coefficients q_i , $i = 1, 2, \dots, M+1$ are sequentially grouped in order, timewise, according to positive or negative values. For example, if q_1 is positive, q_2, q_3 and q_4 negative and q_5 and q_6 positive with q_7 negative then q_1 forms the first group, q_2, q_3 , and q_4 the second group and q_5 and q_6 the third groups, etc. A single spline region is designated to span each group of positive values. The same is true for each series of negative values. The number of groups determine the starting estimate for the minimum number of knots. Let $m+1$ represent the number of such groups.

10.2 A Starting Estimates Procedure for the Knot Locations

The times separating the above groups provide excellent starting estimates for the knot locations. For example, the times

$$t_1 = \widetilde{T}_1$$

$$t_2 = \widetilde{T}_4$$

$$t_3 = \widetilde{T}_6$$

$$\vdots$$

$$t_m = \widetilde{T}_j, \text{ for some } j$$

can be used as excellent starting estimates for the sequence of knots $T_1, T_2, T_3, \dots, T_m$ that are used in the Optimal Spline Method of Chapters VI-IX.

With reference to Equation (4.1) let σ^2 denote the variance of the data to be splined. In the system identification of aircraft the following procedure works well for estimating the minimum of knots and for providing starting estimates of the knot locations. The knots are recursively located so that the RMS value between the data and the spline fit is approximately equal to σ over each spline region. This is accomplished by placing the first knot so that the first spline region is the maximum of all spline intervals that have an associated RMS less or equal to σ . Each succeeding knot is similarly placed.

CHAPTER XI

CONCLUSIONS

An automated technique called the Optimal Spline Method has been developed for application to problems having high nonlinearities. Its application to ship classification and to aircraft system identification has solved a major problem in each of those technological areas. These are: (a) the development of a technique to determine independent features for classification of ship types and (b) the development of a method that minimizes the number of parameters that are necessary for optimal estimation of force and moment time histories in aircraft system identification.

The Optimal Spline Method in ship classification applications determines the number of separate superstructure masses, their separation from each other, their locations and their extended widths. These independent features correspond directly to optimal spline coefficients of the method. The results contained in Chapter II show that ships of like type have similar optimal spline coefficients and ships of different types exhibit large differences in their optimal spline coefficients. In particular, it is shown that the optimal spline coefficients provide a clear distinction between a DLG class and a DDG class.

In aircraft system identification applications the use of the Optimal Spline Method has two advantages. They are: (a) the computations and the storage requirement of the estimation process can be significantly reduced without a decrease in estimation performance and (b) an increase in estimation and, therefore, in identification performances can be achieved under the constraint of a fixed number of spline parameters. Advantage (b) is demonstrated by the results contained in Figures 3-1 through 3-4. Figure 3-4 shows the results of using eight equally spaced knots. The increase in

performance due to the application of the Optimal Spline Method is shown in Figure 3-2. Advantage (a) is indirectly demonstrated by the results contained in Figures 3-1 through 3-4. In Figure 3-2 the third and fourth knots are separated by 0.82 seconds. In order to obtain equivalent performance through the use of equally spaced knots it is necessary to space them at approximately 0.82 seconds. This spacing increases the number of knots from eight to more than sixteen. The computations and the storage requirement increase exponentially with the number of knots.

REFERENCES

1. Stalford, H. L., "Classification of Ships and the General Identification Problem," presented at the NRL workshop on Signal Processing, " May 1, 1975.
2. Schneider, H., "Matched Polynomial Least Squares Fitting and Application to Real Time Ballistic Coefficient Estimation," M.I. T. LL TN-1966-34, July 1966.
- 3.
- 4.
- 5.
- 6.
- 7.
- 8.
9. Schneider, H., and G. Gordon, "Real Time Spline Methods for Non-linear Estimation", presented at the 2nd Symposium on Nonlinear Estimation Theory and Applications, held in San Diego, California, Sept. 13-15, 1971 (U), (published by Western Periodicals Publishing Co.).
10. Schneider, H., "Integral Solutions to a General Class of Nonlinear Estimation and System Identification Problems", presented at the 4th Symposium on Nonlinear Estimation Theory and its Applications, held in San Diego, California, Sept. 10-12, 1973, (published by Western Periodicals Publishing Company).

RE: Classified references-
Delete per Ms. Randall, ONR/Code 432

11. Schneider, H., and P. B. Reddy, "A New Optimization Technique for Solving Nonlinear Two Point Boundary Value Optimal Control Problems with Application to Variable Vector Thrust Atmospheric Interceptor Guidance", AIAA Paper No. 74-827, AIAA Mechanics and Control of Flight Conference, Anaheim, California, Aug. 5-9, 1974.
12. Schneider, H., P. B. Reddy, "Nonlinear Spline Method for Optimal Thrust Vector Control Atmospheric Interceptor Guidance", revision submitted for publication in the AIAA Journal, Jan. 6, 1976.
13. Ramachandran, R., Schneider, H., Mason, J., Stalford, H., "Identification of Aerodynamic Characteristics of a Light Jet Trainer Aircraft at High Angles of Attack and Sideslip from Simulated Flight Data using the EBM Technique, Presented at the 4th AIAA AFM Meeting, August 8-10, 1966, Hollywood, Florida.
14. Leitmann, G., The Optimization of Rocket Trajectories - A Survey Appendix A, in "Progress in the Astronautical Sciences" (S. F. Singer, ed.). North-Holland, Amsterdam, 1962.
15. Edelbaum, Theodore N., Theory of Maxima and Minima, in "Optimization Techniques with Applications to Aerospace Systems" (George Leitmann, ed.). Academic Press, New York, 1962.

UNCLASSIFIED

SECURITY CLASSIFICATION OF THIS PAGE (When Data Entered)

REPORT DOCUMENTATION PAGE		READ INSTRUCTIONS BEFORE COMPLETING FORM
1. REPORT NUMBER	2. GOVT ACCESSION NO.	3. RECIPIENT'S CATALOG NUMBER
4. TITLE (and Subtitle) Optimal Spline Method with Applications to Ship Classification and to Aircraft System Identification		5. TYPE OF REPORT & PERIOD COVERED Final Engineering Technical Rept. 23 July 76- 31 Jan 77
7. AUTHOR(s) Harold L. Stalford and Chan Park		6. PERFORMING ORG. REPORT NUMBER R-227U
PERFORMING ORGANIZATION NAME AND ADDRESS Dynamics Research Corporation 60 Concord Street Wilmington, Mass. 01887		8. CONTRACT OR GRANT NUMBER(s) N00014-76-C-1022
11. CONTROLLING OFFICE NAME AND ADDRESS Office of Naval Research 800 North Quincy Road Arlington, VA 22217		10. PROGRAM ELEMENT, PROJECT, TASK AREA & WORK UNIT NUMBERS 1279
14. MONITORING AGENCY NAME & ADDRESS (if different from Controlling Office) Same		12. REPORT DATE March 1977
		13. NUMBER OF PAGES 75
		15. SECURITY CLASS. (of this report) Unclassified
		15a. DECLASSIFICATION/DOWNGRADING SCHEDULE
16. DISTRIBUTION STATEMENT (of this Report) Distribution of this document is unlimited		
17. DISTRIBUTION STATEMENT (of the abstract entered in Block 20, if different from Report)		
18. SUPPLEMENTARY NOTES		
19. KEY WORDS (Continue on reverse side if necessary and identify by block number) Optimal Spline Method Knot and Parameter Optimization Applicability to Ship Classification Applicability to Aircraft System Identification Newton's Gradient Method Quadratic Convergence		
20. ABSTRACT (Continue on reverse side if necessary and identify by block number) This report describes a method for optimal placement of knots in a quadratic spline representation of nonlinear functions. Newton's gradient method is utilized to obtain quadratic convergence of knot locations. Applications to ship classification and to aircraft system identification are presented.		

DD FORM 1 JAN 73 1473 EDITION OF 1 NOV 65 IS OBSOLETE

SECURITY CLASSIFICATION OF THIS PAGE (When Data Entered)

Distribution List for Technical Report
to Contract N00014-76-C-1022

Office of Naval Research Department of the Navy Arlington, Virginia 22217 ATTN: Dr. S. Brodsky, Code 432	(2)	Scientific Officer Director Mathematics Program Mathematical & Information Sciences Division Office of Naval Research 800 North Quincy Street Arlington, Virginia 22217 ATTN: Dr. L. D. Bram, Code 432	(1)
Commanding Officer Naval Weapons Center China Lake, California 93555 ATTN: Dr. Lonnie Wilson, Code 3158	(1)		
Commanding Officer Naval Air Systems Command Washington, D.C. 20360 ATTN: Ed Hooper, NAIR-370	(1)		
Commanding Officer Naval Electronic Systems Command Washington, D.C. 20360 ATTN: Dr. Franklin W. Diederick, PME106T	(1)		
Air Force Office of Scientific Research-NM Building 410 Bolling AFB Washington, D.C. 20332 ATTN: Capt. Charles Nefzger	(1)		
Commanding Officer Naval Air Development Center Warminster, Pennsylvania 18974 ATTN: Ron Nave	(1)		
Director Naval Research Laboratory Washington, D.C. 20375 ATTN: Code 2627	(6)		
Office of Naval Research Department of the Navy Arlington, Virginia 22217 ATTN: Code 102IP	(6)		
Defense Documentation Center Bldg. 5, Cameron Station Alexandria, Virginia 22314	(12)		
Office of Naval Research Branch Office 495 Summer St. Boston, Mass. 02210	(1)		